

1 **Detection of dimming/brightening in Italy from homogenized all-** 2 **sky and clear-sky surface solar radiation records and underlying** 3 **causes (1959-2013)**

4 Veronica Manara^{1,2}, Michele Brunetti³, Angela Celozzi⁴, Maurizio Maugeri^{1,3}, Arturo Sanchez-
5 Lorenzo⁵, Martin Wild²

6 ¹Department of Physics, Università degli Studi di Milano, Milan, Italy

7 ²ETH Zürich, Institute for Atmospheric and Climate Science, Zürich, Switzerland

8 ³Institute of Atmospheric Sciences and Climate, CNR, Bologna, Italy

9 ⁴Italian Air Force, COMET Centro Operativo per la Meteorologia, Pratica di Mare (RM), Italy

10 ⁵Instituto Pirenaico de Ecología, Consejo Superior de Investigaciones Científicas (IPE-CSIC), Zaragoza, Spain

11

12 *Correspondence to:* Veronica Manara (veronica.manara@unimi.it)

13

14 **Abstract.** A dataset of 54 daily Italian downward surface solar radiation (SSR) records has been set up collecting data for
15 the 1959-2013 period. Special emphasis is given to the quality control and the homogenization of the records in order to
16 ensure the reliability of the resulting trends. This step has been shown as necessary due to the large differences obtained
17 between the raw and homogenized dataset, especially during the first decades of the study period. In addition, SSR
18 series under clear-sky conditions were obtained considering only the cloudless days from corresponding ground-based
19 cloudiness observations. Subsequently, records were interpolated onto a regular grid and clustered in two regions, Northern
20 and Southern Italy, which were averaged in order to get all-sky and clear-sky regional SSR records. Their temporal
21 evolution is presented, and possible reasons for differences between all-sky and clear-sky conditions and between the two
22 regions are discussed in order to determine to which extent SSR variability depends on aerosols or clouds. Specifically,
23 the all-sky SSR records show a decrease until the mid-1980s (dimming period), and a following increase until the end of
24 the series (brightening period) even though strength and persistence of tendencies are not the same in all seasons. Clear-sky
25 records present stronger tendencies than all-sky records during the dimming period in all seasons and during the
26 brightening period in winter and autumn. This suggests that under all-sky conditions the variations caused by the
27 increase/decrease of the aerosol content have been partially masked by cloud cover variations, especially during the
28 dimming period. Under clear-sky the observed dimming is stronger in the South than in the North. This peculiarity could
29 be a consequence of a significant contribution of mineral dust variations to the SSR variability.

30

31 **1 Introduction**

32 The fraction of solar radiation that reaches the Earth's surface is the source of energy which drives the majority of the
33 processes in the atmosphere and in the oceans and plays a crucial role in a large number of sectors (e.g. agriculture,
34 tourism, solar energy production) (Hartmann et al., 1986; Wild, 2009, 2012). For these reasons, it is very important to
35 study the spatial distribution and the temporal behavior of surface solar radiation (SSR). Continuous observations by
36 thermoelectric pyranometers at the Earth's surface date back to 1920s, as for example at the Stockholm site since 1923
37 (Stanhill, 1983; Wild et al., 2009). Surface radiation measurements started to become available on a widespread basis
38 only in the late 1950s, with the establishment of numerous radiation sites during the International Geophysical Year
39 (IGY) 1957-1958.

40 Studies of the last decades demonstrated that SSR has not been constant over time (Dutton et al., 1991; Liepert et al.,
41 1994; Ohmura and Lang, 1989; Russak, 1990; Stanhill and Moreshet, 1992), as shown by decadal fluctuations which
42 exceed the accuracy limit of observational irradiance measurements (2% on an annual basis) (Gilgen et al., 1998). They
43 report a decrease in SSR, “global dimming”, of about $3\text{-}9\text{Wm}^{-2}$ from the 1950s to the 1980s and a subsequent increase,
44 “brightening”, of about $1\text{-}4\text{Wm}^{-2}$ from the beginning of 1980s (Wild, 2012). These two periods are highlighted not only
45 by studies focusing on specific regions (Liang and Xia, 2005; Long et al., 2009; Sanchez-Lorenzo and Wild, 2012;
46 Sanchez-Lorenzo et al., 2013, 2015; Wang and Yang, 2014) but also by studies focusing on worldwide data sets (Alpert
47 et al., 2005; Gilgen et al., 1998; Liepert, 2002; Stanhill and Cohen, 2001; Wang et al., 2012; Wild et al., 2005, 2009).

48 The causes of these decadal variations are not completely clear: it has been suggested that changes in the anthropogenic
49 aerosols and cloud cover can be major causes (e.g., Liepert et al., 1994; Stanhill and Cohen, 2001; Wild, 2009, 2015),
50 while changes in radiatively active gases concentrations have, at least, globally a minor effect (Kvalevåg and Myhre,
51 2007; Romanou et al., 2007). Aerosols and clouds can interact in various ways and are therefore not completely
52 independent (Ramanathan et al., 2001). Aerosols act as a modulator of SSR by absorption or scattering of solar
53 radiation (direct effect) (Radke et al., 1989; Twomey et al., 1984) and by changing the number of cloud condensation
54 nuclei particles (indirect aerosol effect) that also change albedo and cloud lifetime (Albrecht, 1989; Lohmann and
55 Feichter, 2005). The increase of anthropogenic aerosol emissions in the 20th century is thought to be the major cause of
56 the observed decadal SSR reduction until the 1980s (e.g., Liepert and Tegen, 2002; Norris and Wild, 2007; Stanhill and
57 Cohen, 2001), while measures to reduce air pollution in the late 20th century are possibly responsible for the renewed
58 increase of SSR (Chiacchio and Wild, 2010; Dutton et al., 2004, 2006; Hansen et al., 1997; Nabat et al., 2014).
59 Nevertheless, the relative contribution of clouds and aerosols is not clear yet, especially after comparing studies
60 regarding different areas.

61 For these reasons, it is interesting to understand to which extent the SSR variability depends on aerosol variations or on
62 changes in cloud characteristics. Different studies tried to estimate this distinction by using global climate models,
63 satellite-derived products and ground-based observations, finding a good agreement between clear-sky SSR variations
64 and changes in aerosol emissions and concentrations, indicating aerosols as major contributor to SSR variability at
65 decadal scale (Wild, 2015). In addition, some studies analyzing all-sky SSR highlighted the important contribution of
66 clouds especially at interannual scale (Folini and Wild, 2011; Mateos et al., 2014; Norris and Wild, 2007; Parding et al.,
67 2014; Xia, 2010a, 2010b). Other studies confirmed that changes in aerosols play a major role in the decadal variations
68 of SSR (Li et al., 2007; Zhang et al., 2015), although there is a tendency to underestimate the dimming and brightening
69 obtained with models with respect to trends obtained with ground-based observations. This has been attributed to
70 possible deficiencies in aerosol emission inventories or an underestimation of aerosol direct radiative forcing (Allen et
71 al., 2013; Cherian et al., 2014; Folini and Wild, 2011; Ruckstuhl and Norris, 2009). As far as the aerosol radiative
72 forcing is concerned, some studies tried to analyze the problem combining SSR series with optical depth and aerosol
73 concentration observations finding a comparable or higher contribution of the direct aerosol effect with respect to the
74 indirect aerosol effect (Nabat et al., 2014, 2015; Ohmura, 2009; Ruckstuhl et al., 2008; Turnock et al., 2015). However,
75 few studies used only ground-based observations to obtain clear-sky and all-sky SSR series in order to investigate the
76 aerosol-cloud effect (Liang and Xia, 2005; Liepert, 2002; Long et al., 2009; Ruckstuhl et al., 2008; Wild et al., 2005);
77 this is due to the difficulty in recovering high temporal resolution SSR series together with additional information on
78 cloudiness or direct/diffuse radiation to discriminate clear-sky conditions (Long and Ackerman, 2000; Wild, 2009).

79 In Italy, studies on the temporal evolution of SSR and on its relation to aerosol concentrations and cloud cover
80 variability are not available. The best available information concerns sunshine duration (SD) for the 1936-2013 period

81 (Manara et al., 2015). It shows an increasing tendency starting in the 1980s preceded by a less evident decreasing
82 tendency. Comparing these trends with corresponding cloud amount series, Manara et al., (2015) found that the
83 expected negative correlation of these two variables is often not evident. This suggested that during the global
84 dimming/brightening periods there is an important fraction of SD evolution that cannot be explained by cloud cover
85 changes which must therefore depend on other factors such as, for example, changes in aerosol optical thickness. The
86 temporal variations of aerosol optical thickness of the last decades seem to be mainly driven by anthropogenic
87 emissions (Streets et al., 2006, 2009), even though, especially for Southern Italy, also mineral particles originating from
88 Sahara and Sahel areas may have a significant role, as recently suggested for Spain by Sanchez-Romero et al. (2016).
89 This natural atmospheric aerosol, with emissions that are highly variable from year to year, is a significant component
90 of the Mediterranean area (Pey et al., 2013; Varga et al., 2014) causing reflection and absorption of the incoming solar
91 radiation and therefore affecting the energy balance together with anthropogenic aerosols (Zhu et al., 2007).
92 In this context, this work aims at collecting, quality checking, homogenizing (Sect. 2) and analyzing an extensive
93 database of Italian SSR records in order to obtain average regional series both under all-sky (Sect. 3.1) and clear-sky
94 conditions (Sect. 3.2). By doing this, we want to describe how SSR has changed in Italy during about the last sixty years
95 and to explain how these variations depend on aerosols or cloud variability (Sect. 3.3, Sect. 4).

96

97 **2 Data and data-preprocessing**

98 **2.1 Data**

99 The Italian SSR series used in this work were obtained at daily scale from the Italian Air Force stations (AM –
100 Areonautica Militare, 29 series – 1959-2013 period) and from the National Agro-meteorological Database (BDAN –
101 Banca Dati Agrometeorologica Nazionale, 19 series – 1994-2013 period). Some information about the history of the
102 AM observations are available in a report of the Italian Air Force (2012) and the data for the 1964-2013 period are also
103 available in the World Radiation Data Centre (WRDC) of the Main Geophysical Observatory in St. Petersburg. In order
104 to increase data availability, especially for the alpine region, we considered also the series from the meteorological
105 observatory of Trieste (1971-2013 period) (Stravisi and Cirilli, 2014) and five series from Switzerland, close to the
106 Italian border, from the Swiss Federal Office of Meteorology and Climatology (MeteoSwiss – 1981-2013 period).

107 The data that come from the AM stations and from the meteorological observatory of Trieste were recorded with the
108 Robitzsch bimetallic actinography until the 1980s. This instrument was then replaced with the CM11 Kipp & Zonen
109 pyranometer in the first case and with different types of CM Kipp & Zonen pyranometer in the second one (for more
110 details about AM instruments and instrument changes see: <http://wrdc.mgo.rssi.ru/>, while for more details about Trieste
111 instruments see Stravisi, (2004)). The CM11 Kipp & Zonen pyranometer was also used in the stations included in the
112 BDAN database with the only exception of two stations that used the EP07 Middleton Instruments pyranometer.
113 Finally, the data that come from MeteoSwiss were measured with a CM21 Kipp & Zonen pyranometer.

114 The main difference between the Robitzsch bimetallic actinography and the Keep & Zonen pyranometer is that in the
115 first case the measure is mechanic while in the second one it is thermoelectric. Specifically, the Robitzsch pyranometer
116 consists of a black metallic strip located between two white metallic strips. Due to differential absorption, a temperature
117 difference is created between the strips which serves as a measure of radiation intensity. This temperature difference
118 drives the position of a pen which allows recording radiation intensity on a paper strip chart. The sensitivity range
119 covers the entire spectrum of solar radiation; only radiation above $2\mu\text{m}$ is not included, this, however, contributes only
120 very little to the solar irradiance.

121 The Kipp & Zonen and Middleton Instruments pyranometers are based on a black-coated surface which is warmed up
122 by solar radiation. The thermal energy is converted into measurable voltage which is used to measure the solar
123 irradiance. These pyranometers are provided with an automatic acquisition system which allows recording solar
124 irradiance on a digital support. The spectral range covers the interval 0.3-2.8 μ m.

125 The final data set is composed of 54 daily series with data for the 1959-2013 period. All series have at least 15 years of
126 data (Fig. 1 and Table 1). The spatial distribution of the stations and the length of the series in relation to their location
127 is uniform, the only exception are the series in the Alps and Apennines. All series are located in the plains and coastal
128 areas with elevation lower than 600m. Data availability versus time is rather inhomogeneous with a minimum before
129 the beginning of the period covered by the BDAN series (Fig. 2).

130 **2.2 Data homogenization, gap-filling and anomaly records**

131 Before analyzing the time evolution of SSR, we subjected the records to a quality check and to a homogenization
132 procedure. Quality check was performed at a daily time-scale in order to find out and correct gross errors (Aguilar et al.,
133 2003). Specifically, we searched for negative values and values exceeding the radiation at the top of the atmosphere. In
134 addition, the reliability of station coordinates was checked by means of the comparison with station metadata and
135 checking the elevation in relation to position. After quality check, monthly series were calculated when the proportion
136 of missing data did not exceed 20%.

137 All monthly records were subjected to homogenization in order to identify and eliminate non climatic signals (Aguilar
138 et al., 2003; Brunetti et al., 2006b). Our aim was to identify time-dependent adjusting factors in order to transform the
139 original records into homogeneous ones. The homogenization of the series was performed using a procedure based on a
140 relative homogeneity test (Brunetti et al., 2006b) based on statistical methods supported by metadata information.
141 Specifically, each test series is compared against 10 other reference series that well correlate with the test one by means
142 of the Craddock test (Craddock, 1979). This methodology is suitable to calculate correcting factors, but the
143 identification of an inhomogeneity is not always easy and unambiguous (Brunetti et al., 2006b). For this reason, we
144 homogenize a period only when more reference series give coherent adjustment estimates. In this way, we can be more
145 confident that the inhomogeneity is “real” and ascribable to the test series and not to the reference series. The reference
146 series that result homogeneous in a sufficiently long-sub-period centered on the break year are then selected to estimate
147 the adjustments. We use several series to estimate the adjustments to increase their stability and to avoid unidentified
148 outliers in the reference series from producing wrong corrections. By comparing the obtained breaks of each series with
149 the corresponding metadata, we found in most of the cases a reasonable agreement between the breaks identified by the
150 statistical method with information reported by metadata.

151 The common variance between two stations depends on their distance and for the Italian territory, as previously found
152 for SD (Manara et al., 2015), it falls to 50% at a distance of about 150 km. Homogenization was performed in a
153 monthly time scale. However, a daily version of the adjustments was also generated in order to homogenize the daily
154 series.

155 All analyzed series showed at least one inhomogeneous period highlighting the importance of homogenization,
156 especially before 1980. The most relevant inhomogeneities fall in the first 20 years of the investigated period where
157 many instrument changes and recalibrations occurred, whereas the inhomogeneities are less relevant from the 1980s
158 when the Robitzsch pyranograph was replaced in all AM stations by the CM11 Kipp & Zonen pyranometer (Table 1),
159 an instrument with higher quality, as recommended by WMO (Italian Air Force, 2012).

160 Figure 3a shows the Italian average annual SSR anomaly series (relative anomalies with respect to the period 1976-
161 2005) before and after homogenization with corresponding Gaussian low-pass filters (11-year window; 3-year standard

162 deviation) that allow a better visualization of the decadal variability and long-term trend, while Fig. 3b shows the curve
163 obtained by averaging the mean annual adjustments over all single records, together with their absolute range. The
164 details on how we obtained regional SSR anomaly series will be explained in the following sections.

165 The average annual records before and after the homogenization show a different decadal variability during the 1959-
166 1970 and 1971-1980 periods where increasing (average adjustment: 1.098) and decreasing (average adjustment: 0.964)
167 correcting factors, respectively, have been applied to the original series. On the contrary, during the 1981-2013 period
168 the two series show a similar behavior, where in fact only small correcting factors have been applied to the original
169 series (average adjustment: 1.008). Overall, the use of the raw series hides the trends obtained during the study period,
170 especially before the 1980s when the dimming period observed in the homogenized series is not evident during the
171 1960s and early 1970s.

172 We filled the gaps in each monthly record using a procedure similar to that described in Manara et al. (2015). In
173 particular, the median of a set of five estimated values, corresponding to the five highest correlated reference records,
174 was selected in order to avoid outliers resulting from peculiar climatic conditions of the reference station. When less
175 than five reference records fulfilling the requested conditions (distance within 500 km from the record under analysis
176 and at least six monthly values in common with it in the month of the gap) were available, the median was calculated
177 with the available reference series. After the gap filling procedure, all series had at least 90% of available data during
178 the 1959-2013 period and 99% during the 1976-2005 period (Fig. 2), used as reference period to calculate the anomaly
179 series. So, all the series were transformed into monthly/seasonal/annual relative anomaly series with respect to the
180 monthly/seasonal/annual 1976-2005 normals. Seasons are calculated according to the following scheme: December-
181 January-February (winter), March-April-May (spring), June-July-August (summer), September-October-November
182 (autumn) and the year is calculated for the December-November period. The winter season is dated to the year in which
183 January and February fall and, for the first year, the winter and the annual means are calculated using also the monthly
184 mean of December 1958.

185 **2.3 Gridding and regional average record**

186 Starting from the monthly/seasonal/annual anomaly series, we generated a gridded version of the anomaly series with a
187 resolution of $1^\circ \times 1^\circ$ in order to balance the contribution of areas with a higher number of stations with the contribution
188 of areas with a lower number of stations. This technique, explained in more detail by Brunetti et al. (2006b) and Manara
189 et al. (2015), is based on an Inverse Distance Weighting approach with the addition of an angular term to take into
190 account the anisotropy in the spatial distribution of stations. The resulted grid spans from 7° to 18° E and from 37° to
191 47° N, with 58 grid points over the Italian territory (Fig. 1).

192 Then, the monthly gridded anomaly records were subjected to a Principal Component Analysis (PCA) in order to
193 identify areas with similar SSR temporal variability. With this technique, it is possible to identify a small number of
194 variables, which are linear functions of the original data and which maximize their explained variance (Preisendorfer,
195 1988; Wilks, 1995). The analysis focused on the 1976-2005 period, the same reference period used to calculate the
196 anomaly series. The analysis shows that the first five eigenvectors have an eigenvalue greater than 1 and they explain
197 more than 91% of the total variance of the data set. Then, we selected to rotate the first two empirical orthogonal
198 functions (EOFs), which are those that account for 59% and 23% respectively of the original variance of the data set, in
199 order to obtain a more physically meaningful pattern (Von Storch, 1995). We decided to select these two EOFs because
200 they account for 82% of the original variance while the other three account only for 9%. This procedure allowed to
201 divide the Italian territory in two regions: Northern Italy (29 grid points) and Southern Italy (29 grid points) (Fig. 1).
202 Finally, we calculated the monthly, seasonal and annual mean anomaly series for the two regions by averaging all

203 corresponding grid point anomaly records. From here, we refer to these series as the SSR anomaly series obtained under
204 all-sky conditions to distinguish them from the series presented in the next section (Sect. 2.4) obtained selecting only
205 the clear-sky days.

206 **2.4 Clear sky series**

207 Starting from the 54 homogenized daily SSR series presented in Sect. 2.1 and in Sect. 2.2, we aimed at determining
208 clear SSR days for the 1959-2013 period. For this purpose, we used an updated version (both for number of series and
209 series length) of the total cloud cover (TCC) database presented by Maugeri et al. (2001) as reference to extract the
210 clear-sky days. In particular, we considered only the days with a daily TCC mean of 0 okta. For the SSR series without
211 a corresponding TCC series, we considered the data from nearby stations. The main limitation of the previous procedure
212 is that the condition adopted to select clear-sky days (0 okta of TCC) allows often to select a very low number of days.
213 We tried therefore to apply a less restrictive condition and we extracted also the clear-sky days using as threshold 1
214 okta. The average of clear-sky days per station and month is 9% for the 0-okta threshold and 18% for the 1-okta
215 threshold. These fractions are however higher in summer when SSR is more important, reaching the maximum value in
216 July with 17% of 0-okta days and 34% of days with less than 1-okta of TCC.

217 Then, the monthly mean was calculated when at least two clear-sky daily values were available in the considered
218 month. After gap-filling, the monthly/seasonal/annual relative anomaly series were obtained with respect to the 1976-
219 2005 period using the same technique explained in Sect. 2.2. To calculate the anomaly series we considered only the
220 series with at least 50% (for 0 okta) and 80% (for 1 okta) of available data in the 1976-2005 period after the gap-filling.
221 This reduced the series to 44 in the first case (Table 1). As final step, we interpolated the anomaly series as described in
222 Sect. 2.3 and we obtained the regional anomaly series, for the two regions and the two thresholds, by averaging all
223 corresponding grid point anomaly series.

224

225 **3 Results**

226 **3.1 Trend analysis of the all-sky SSR records**

227 The average Northern and Southern Italy annual and seasonal SSR records obtained under all-sky conditions are shown
228 in Fig. 4, together with the same low-pass filter used in Fig. 3. In order to better understand the depth and the length of
229 the tendencies showed in Fig. 4, we subjected the records to a running trend analysis (Brunetti et al., 2006a) estimating
230 the trend slope of each sub-interval of at least 21 years by applying a linear regression. The results are shown in Fig. 5.
231 Specifically, we represent the length of the period considered for the analysis (y axes) in relation to the starting year of
232 the window that the trend refers to (x axes). Slopes are shown by means of the colors of the corresponding pixels with
233 large squares for trends with a significance level $p \leq 0.1$ and with small squares for trends with a significance level
234 $p > 0.1$ considered here non statistically significant, with significance levels estimated by means of the Mann-Kendall
235 non parametric test (Sneyers, 1992).

236 At annual scale both regions show a decreasing tendency until the mid-1980s and a following increase until the end of
237 the series, with a period of stabilization in the late 1990s. The trends of the two periods are comparable, especially in
238 the Southern region. In fact, the trend for the whole period under analysis (e.g., 1959-2013 period) is not statistically
239 significant, as highlighted by the running trend analysis (Fig. 5). However, the intensity of the dimming is slightly
240 higher for the South than the North, especially for some windows starting in the mid-1960s (e.g., about -3% per decade
241 for the North and about -4% per decade for the South for the 1965-1985 period), while the brightening is more intense
242 in the North especially for the windows starting in the mid-1980s (e.g., about +4% per decade for the North and about
243 +2% per decade for the South for the 1980-2010 period).

244 For the winter season, the records show a well-defined behavior with a dimming and a following brightening only in the
245 Northern region where the record shows statistically significant negative and positive tendencies for some periods
246 starting in the 1960s and 1980s, respectively. On the contrary, the behavior is not well defined in the Southern region,
247 with a minimum in the mid-1980s and two secondary maxima during the 1970s and 1990s (Fig. 4). As a consequence,
248 the series shows only some sub-periods with a statistically significant trend. They are less than 35 years long and they
249 start in the 1960s with negative sign and in late 1970s/early 1980s with positive sign. There is also a window extending
250 21 years starting in 1990 with a significant decreasing tendency (-4% per decade) (Fig. 5).

251 The spring season has a similar pattern to the annual one with a clear negative-positive sequence and a period of
252 stabilization during the second half of 1990s both for Northern and Southern Italy. The records show a comparable
253 dimming for the two regions for periods longer than 30 years with variations of about -3% per decade (e.g. 1962-1992
254 period), while it is slightly stronger in the North if sub-periods starting in the mid-1960s with less than 30 years are
255 considered in which variations range between -7% and -5% per decade. As far as the brightening is concerned, it is
256 stronger in the Northern region, both for long and short sub-periods with values of about +6% per decade for some
257 windows starting in the 1980s.

258 For the summer season the sequence of the dimming and brightening is evident and very similar to the annual and
259 spring behavior only in the South. In the North, during the dimming period, there are only very few sub-periods with a
260 significant decreasing trend, while in the South the most part of the windows starting in the 1960s have significant
261 trends with variations of about -3% per decade (e.g. 1960-1990 period) indicating a reduction of SSR. On the contrary,
262 the brightening period is quite comparable for the two regions and reaches values of about +4% per decade (e.g. 1983-
263 2013 period). The trends of the longest periods are significant and positive with values of about +1% per decade (e.g.
264 1959-2013 period) only in the North as a consequence of its weaker dimming in the early period.

265 The autumn records (Fig. 4) start with a period without any trend for both regions and then they show a decrease
266 between the beginning of 1970s and the beginning of 1990s and a following increase, which is stronger in the Northern
267 than in the Southern region. This picture is evident also in the running trends (Fig. 5), especially for the brightening
268 period where some sub-periods have a positive trend after the beginning of the 1980s in the North and none has a
269 positive trend in the South with the only exception of one 21-year sub-period starting in the 1990s. On the contrary most
270 of the sub-periods starting in the 1960s and 1970s have significant and negative trends with values of about -3% per
271 decade. The trend over the whole period under analysis (1959-2013 period) is significant and negative for both regions
272 with values of about -2% per decade.

273 In order to give a more accurate information on the variations highlighted by Fig. 4 and Fig. 5, we estimated the trends
274 in Wm^{-2} per decade for some key periods (Table 2), including 1959-2013 (the entire period covered by the records),
275 1959-1985, 1986-2013 (the dimming and brightening periods according to the Northern and Southern Italy annual
276 records) and other periods to allow a direct comparison with some relevant dimming/brightening papers (Sanchez-
277 Lorenzo et al., 2015; Wild, 2012). Specifically, we calculated the absolute series for each grid-point multiplying each
278 seasonal/annual anomaly series obtained under all-sky conditions by the corresponding seasonal/annual normals and
279 then we calculated the seasonal and annual regional records, by averaging all corresponding grid point absolute series.
280 The seasonal/annual normals were calculated by averaging the corresponding monthly normals obtained using the same
281 data and the procedure explained by Spinoni et al. (2012). In particular, the monthly normals were obtained starting
282 from a database of SD normals for the Italian territory referring to flat and non-shaded sites. These normals were first
283 transformed into SSR normals by means of the Ångström law and then interpolated onto the USGS GTOPO 30 Digital
284 Elevation Model grid (USGS, 1996) by means of an Inverse Distance Gaussian Weighting spatialization model.

285 As previously shown, the trend over the whole period under analysis (1959-2013) is significant only in summer in the
286 North ($+3.1\text{Wm}^{-2}$ per decade) and in autumn for both regions (-1.5Wm^{-2} and -2.2Wm^{-2} for the North and the South
287 respectively). In the first case, considering the weak (and not significant) dimming, the trend over the whole period is
288 mostly driven by the increasing tendency of the second period while in the second case, considering the weak
289 brightening, the trend over the whole period is mostly driven by the decreasing tendency of the first period. Considering
290 the 1959-1985 period, as reference for the dimming period, the trend is significant in all the seasons both for the North
291 and the South with values ranging between -7.2Wm^{-2} per decade in spring and -3Wm^{-2} per decade in winter for the
292 North and between -8.5Wm^{-2} per decade in spring and -4.2Wm^{-2} per decade in autumn for the South. As far as the
293 brightening period is concerned, considering the 1986-2013 period, the trend is significant in all the seasons in the
294 Northern region with values ranging between $+3.2\text{Wm}^{-2}$ per decade in winter and $+12.3\text{Wm}^{-2}$ per decade in summer,
295 while in the Southern region it is significant only at annual scale and during spring ($+7.6\text{Wm}^{-2}$ per decade) and summer
296 ($+13.5\text{Wm}^{-2}$ per decade).

297 **3.2 Trend analysis of the clear-sky SSR records**

298 The average Northern and Southern Italy seasonal and annual SSR records obtained under clear-sky conditions using 0
299 okta and 1 okta as thresholds to select the clear days are shown in Fig. 6. The correlations between the records obtained
300 with the two thresholds are comprised between 0.86 for the spring season and 0.97 for the winter season in the North
301 and between 0.87 for the winter and autumn season and 0.95 for the summer season in the South. The agreement
302 increases if the correlation between the filters is considered (it is always higher than 0.96). The decadal variability
303 shown by the trends using the two thresholds is very similar with the exception of few periods where one of the two
304 records shows a higher interannual variability causing slight differences in the resulting trends. This is evident for
305 example before the 1980s during the spring season in the North and during the winter season in the South; in both cases
306 the 0 okta series shows higher variability than the 1 okta series. The difference in the resulting variability over the
307 whole period under analysis (1959-2013) is particularly evident in the North where it is always higher in the 0 okta than
308 in the 1 okta series (the standard deviation of the residuals from the low-pass filter is comprised between 0.02 and 0.04
309 for the 0 okta series and between 0.01 and 0.03 for the 1 okta series), while it is less evident in the South where the two
310 series show the same variability (the standard deviation of the residuals from the low-pass filter is comprised between
311 0.02 and 0.05 for both the thresholds). The advantage of 0 okta as threshold is that it allows to select only the real clear-
312 sky conditions but the limitation of this choice is that it allows to select only a low number of days (in the North it is
313 particularly due to the higher frequency of cloudy days), thereby increasing the variability of the obtained series. On the
314 contrary using 1 okta as threshold allows to obtain a more stable series selecting a higher number of days, which are
315 however not completely clear.

316 In order to better understand the magnitude and the length of the tendencies shown in Fig. 6, we subjected the clear-sky
317 records to a running trend analysis (Brunetti et al., 2006a), as previously illustrated for the all-sky series. The running
318 trend obtained for the two different thresholds is very similar, so we show and discuss only the one obtained with 0 okta
319 as threshold (Fig. 7).

320 At annual scale the clear-sky records show a comparable decreasing and following increasing tendency both for the
321 North and the South as highlighted by the lack of a significant trend for the whole period under analysis (e.g., 1959-
322 2013 period). However, the dimming period is slightly stronger in the Southern region, especially if the sub-periods
323 with less than 30 years and starting before the 1970s are considered (e.g., about -4% per decade for the South and about
324 -3% per decade for the North for the 1961-1991 period), while the brightening period is slightly more intense in the

325 Northern region (e.g., about +4% per decade for the North and about +3% per decade for the South for the 1981-2011
326 period).

327 During the winter season trends show a dimming and a subsequent brightening for both regions. The dimming is
328 slightly stronger than the brightening and, as a consequence, the trend over almost the whole period under analysis is
329 negative (e.g., -2% per decade during the 1959-2009 for both regions). Records show a period of stabilization during
330 the mid-1970s and during the 2000s (Fig. 6) and, so some sub-periods especially in the South do not show a significant
331 trend after the beginning of 1980s.

332 The spring season has a similar pattern to the annual one with a clear negative-positive sequence after a starting period
333 without any significant trend and a period of stabilization in the 1990s, both for Northern and Southern Italy. The
334 dimming period is stronger in the South than in the North where all the sub-periods with less than 30 years and starting
335 before 1970 show a significant trend with values comprised between -8% per decade and -3% per decade. On the
336 contrary, the brightening period is slightly stronger in the North especially after the mid-1980s with values reaching
337 +6% per decade.

338 During the summer season the two regions show a different trend with a stronger dimming period in the South than in
339 the North (e.g., about -3% per decade for the South and about -2% per decade for the North for the 1961-1991 period)
340 and a stronger brightening period in the North, with all the sub-periods with less than 30 years showing a significant
341 trend. Summer in the North is the only season that shows a significant positive trend for the longest window (e.g., +1%
342 per decade for the 1959-2013 period) while the summer season in the South, that shows a very similar behavior to the
343 annual series, shows a negative trend for the windows that cover almost the whole period under analysis (e.g., -2% per
344 decade for the 1959-2009 period).

345 For the autumn season trends show a decrease until the mid-1980s followed by an increase until the end of the series in
346 both regions, even if in the North a period of stabilization is observed during 1970s as already highlighted by the winter
347 trend. The dimming period is stronger in the South than in the North (e.g., about -5% per decade for the South and
348 about -4% per decade for the North for the 1961-1991 period), while the brightening is stronger in the North even if a
349 period of stabilization is observed during 1990s as already highlighted by the winter trend (e.g., about +4% per decade
350 for the North and about +3% per decade for the South for the 1981-2011 period). Overall, in the northern region the
351 trends of the two periods are comparable while in the South the trend is stronger in the dimming period than in the
352 brightening period resulting in a significant negative trend over the whole period under analysis (e.g., about -2% per
353 decade for the 1959-2013 period).

354 **3.3 Comparison between all-sky and clear-sky SSR records**

355 In order to better investigate the differences between the trends illustrated in Sect. 3.1 and in Sect. 3.2 and so to
356 determine to which extent SSR variability depends either on cloud or on aerosol variability, we compared the annual
357 and seasonal low-pass filter series for all-sky and clear-sky conditions (considering 0 okta as threshold) as shown in Fig.
358 8. For clarity, only filters of the time series are indicated.

359 The comparison between the trends obtained under the two different conditions shows that without the contribution of
360 clouds, dimming and brightening become more intense and significant in all seasons both for North and South. The
361 differences are particularly evident during winter and autumn seasons. Specifically, considering the winter season for
362 both regions, the dimming period is more intense under clear-sky conditions than under all-sky conditions with a
363 significant trend for almost all sub-periods starting before the mid-1970s (see Fig. 5 and Fig. 7). As far as the
364 brightening period is concerned, in the Northern region it is comparable under clear and all-sky conditions if the trend
365 intensity is considered while it presents some differences if curve shapes are taken into account. On the contrary, in the

366 Southern region the brightening becomes stronger and significant under clear-sky conditions even if a period of
367 stabilization is evident in the mid-1990s. After removing cloud contribution, during autumn season the length and
368 intensity of dimming and brightening periods change for both regions. This is due to a shift in the trend inversion from
369 the beginning of 1990s in the North and the end of 1990s in the South to the mid-1980s as already observed for the
370 other seasons both for all-sky and clear-sky conditions. This shift causes a shorter dimming period and a longer and
371 more significant brightening period.

372 Differences between all-sky and clear-sky trends are less evident in spring and summer. Nevertheless, some differences
373 are relevant in both seasons especially during summer in the North where under all-sky conditions there is only a weak
374 decrease while it becomes more intense and significant under clear-sky conditions.

375 The differences between the all-sky and clear-sky anomaly records are highlighted also considering the ratios between
376 the latter and the former records. Before 1980 low-pass filters applied to these ratios (figures not shown) show values
377 higher than one in all seasons with the only exception of autumn. Also at annual scale ratios are higher than one before
378 about 1980 with maxima, of 1.025 in the North (1967) and 1.024 in the South (1968) with a clear decrease in the 1970s.
379 These results seem to suggest that in Italy global dimming has been partially hidden by a decreasing tendency of
380 cloudiness and that without these changes in cloudiness the decrease in SSR in the dimming period would have been
381 greater.

382 The comparison between clear-sky and all-sky anomaly records allows also to quantify the effect of cloudiness on the
383 observed SSR trends and so the effect due to other factors. In this case, we have assumed that if cloudiness did not
384 change, clear-sky and all-sky anomaly records would have had the same behaviour. With this hypothesis virtual
385 constant-cloudiness SSR trends were estimated transforming, by means of the all-sky normals already presented in Sect.
386 3.1, the trends of the clear-sky anomaly records (obtained with 0 okta as threshold) into constant-cloudiness all-sky
387 absolute trends. Trends expressed in Wm^{-2} per decade for the same periods considered in Table 2 for the all-sky series
388 were calculated and the results are reported in the same table.

389 These values confirm what has already been highlighted by Fig. 8. Assuming no changes in cloudiness, at the annual
390 scale the trend during the dimming period (1959-1985) decreases to $-6.3Wm^{-2}$ per decade in the North and to $-8.4Wm^{-2}$
391 per decade in the South (the corresponding all-sky trends are -4.4 and $-6.4Wm^{-2}$ per decade, respectively), confirming
392 that the variations of cloudiness partially masked the all-sky decreasing trends. On the contrary, the influence of the
393 cloudiness variability is not evident during the brightening period (1986-2013) in the North where the all-sky and
394 estimated constant-cloudiness records have almost the same trend, while it is more important in the South where the
395 trend increases from $+6.0Wm^{-2}$ per decade (all-sky) to $+7.9Wm^{-2}$ per decade (estimated constant-cloudiness). This
396 behaviour reflects the variations observed during winter, spring and summer. During autumn the cloudiness variability
397 influenced in a significant way both periods and regions. In particular, during the brightening period the trend changes
398 in the North from $+4.8Wm^{-2}$ per decade (all-sky) to $+6.5Wm^{-2}$ per decade (estimated constant-cloudiness) and in the
399 South from a not significant value (all-sky conditions) to $+5.4Wm^{-2}$ per decade (estimated constant-cloudiness).

400 Without cloud contribution, the correlation between North and South becomes higher: the correlation coefficients range
401 from 0.53 (winter) to 0.78 (year) under all-sky conditions and from 0.67 (autumn) to 0.86 (year) under clear-sky
402 conditions. The largest variation is observed in winter, the season more affected by clouds, where the correlation
403 coefficient increases from 0.53 (all-sky) to 0.84 (clear-sky) while the smallest variation is observed in summer where
404 the correlation coefficient changes from 0.74 (all-sky) to 0.76 (clear-sky). Under all-sky conditions the correlation
405 between the two regions is higher in spring (0.64 for anomalies and 0.94 for filters) and summer (0.74 for anomalies

406 and 0.89 for filters) while under clear-sky conditions the correlation is higher in winter (0.84 for anomalies and 0.96 for
407 filters).

408

409 **4 Discussion and conclusions**

410 A new dataset of long-term Italian SSR records has been set up collecting data from different sources. Particular
411 emphasis is placed upon the quality control and the homogenization of the records in order to ensure the reliability of
412 the resulting trends, which can be affected by non-climatic signals. The majority of the inhomogeneities detected in the
413 series happen before 1980, when many recalibrations, changes in instruments and station relocations occurred, while
414 they become less relevant in the subsequent period. This is also highlighted by the Italian annual mean series where the
415 dimming observed in the homogenized series is not evident in the raw series during the 1960s and early 1970s, showing
416 how at regional level systematic biases in the original records can hide a significant part of the long-term trend.

417 Starting from the homogenized daily records, besides SSR series under all-sky conditions, SSR series under clear-sky
418 conditions were also obtained selecting clear days from corresponding ground-based TCC observations. Then, these series
419 were projected onto a regular grid ($1^\circ \times 1^\circ$) covering the entire Italian territory and clustered in two regions (Northern
420 and Southern Italy) by means of a Principal Component Analysis. The records of these areas were averaged in order to
421 get the corresponding regional all-sky and clear-sky SSR records for the 1959-2013 period.

422 The clearest feature of the Italian all-sky SSR is a significant dimming from the beginning of the series to the mid-
423 1980s and a subsequent brightening until the end of the series for the annual mean, as well as during winter and spring
424 in the Northern region and spring and summer in the Southern region. The trend over the whole period (1959-2013) is
425 significant only during summer (positive) in the North and during autumn (negative) for both regions, as a consequence
426 in the first case of a very weak dimming and in the second one of a very weak brightening.

427 In the clear-sky SSR records, dimming and brightening trends become stronger and they are significant for all seasons
428 and for both regions. The strength of the clear-sky trends is higher than that observed for the all-sky records especially
429 during winter in the South and during summer in the North. The most evident differences between all-sky and clear-sky
430 series are observed in autumn for both regions where not only the variations become more intense and significant but
431 also the change point from dimming to brightening moves from the mid-1990s to the mid-1980s. So, the fact that the
432 change point under all-sky and clear-sky conditions differs by several years in autumn and the intensity of the two
433 periods changes in all seasons supports the hypothesis that clouds contribute in a significant way to the SSR variability
434 under all-sky and confirms the hypothesis formulated by Manara et al. (2015) for SD, suggesting that cloud cover
435 variations have partially masked the dimming caused by the increasing aerosol concentration, especially in the Northern
436 region. This is also confirmed by Maugeri et al. (2001) who found a highly significant negative trend in TCC all over
437 Italy during the period 1951-1996.

438 The resulting trends without the contribution of the clouds show a more coherent pattern over the Italian territory. The
439 peculiarities of a very weak dimming in summer for the North and a very weak brightening in winter for the South, as
440 well as a strong and long dimming in autumn for both regions and the subsequent absence of brightening, are in fact
441 attenuated under clear-sky conditions. The resulting trends under clear-sky conditions for both regions are in agreement
442 with the changes in aerosol and aerosol precursor emissions that occurred during the period under analysis. More
443 specifically, in Italy sulphur dioxide emissions which can be converted to sulphate aerosols show an increasing
444 tendency until the 1980s due to the combustion of solid and liquid fuels (Mylona, 1996) and a decreasing tendency in
445 the following years (Maggi et al., 2006; Vestreng et al., 2007). In parallel, the trends of black carbon and particulate
446 organic matter show a change of tendency starting in the mid-1970s, earlier with respect to the sulphate aerosols due to

447 the reduction of the coal use in residential and commercial sectors as well as improved diesel engines (Novakov et al.,
448 2003). So, the combination of these trends could explain to some degree the SSR variability under clear-sky conditions
449 suggesting anthropogenic aerosols as a relevant contributor of SSR variations in Italy under clear-sky conditions.

450 The dimming in the South in spring, summer and autumn is stronger than in the North under clear-sky and this fact may
451 challenge the above hypothesis as the North is more affected by air pollution due to higher emissions. Nevertheless,
452 Southern Italy is more affected by coarse aerosols (Bonasoni et al., 2004), causing a significant contribution of natural
453 aerosols to SSR variability as for example mineral dust intrusions from the Sahara and Sahel (Prospero, 1996). In
454 particular, we highlight that a comparison between the Northern and Southern Italian clear-sky SSR variations and the
455 Sahel Precipitation Index shows a good agreement, especially in Southern Italy and during the Sahel rainy season
456 (summer and autumn). The correlation coefficients between these two variables over the period 1959-2013 are 0.85 and
457 0.79 for the South and 0.74 and 0.79 for the North, respectively for the summer and autumn seasons suggesting a
458 possible connection between SSR and Sahel Precipitation Index variability. They show a similar behavior with a
459 decreasing tendency from the beginning of the series until the mid-1980s and an increasing tendency in the following
460 period. The results are also coherent with the fact that mineral dust transportation from North Africa into Europe shows
461 a pronounced seasonal cycle with a maximum in summer and a minimum in winter (Pey et al., 2013; Varga et al., 2014)
462 and a distinct gradient with the highest values near the northern coast of Africa (Gkikas et al., 2013; Prospero, 1996).

463 Long-term variations of dust transport into Europe are confirmed by measurements of dust accumulation in Alpine
464 snow, which show a clear increase of mineral dust since the early 1970s with quite high values after the 1980s. This
465 suggests an increase of dust mobilization and transport from North Africa to the north across the Mediterranean and into
466 Europe (De Angelis and Gaudichet, 1991; Maggi et al., 2006) during the first part of the period covered by the SSR
467 series. All this information supports the hypothesis that mineral dust contributes in a significant way to the SSR
468 variability with a higher contribution in the Southern part of Italy than in the Northern part especially during summer
469 and autumn. This could also explain why the summer correlation between the North and the South remains low even
470 under clear-sky conditions, suggesting that cloud cover is not the cause of this low correlation, thus pointing to a
471 different source, such as dust transport, that affects the two regions in a different way. On the contrary, the stronger
472 dimming observed in the North during winter could be a consequence of higher concentrations of anthropogenic
473 aerosols in that region with respect to the South. However, in order to confirm all these hypotheses on the role of natural
474 and anthropogenic aerosols there is need for a better understanding of the factors influencing dust generation and
475 transport and a better understanding of the spatial distribution and temporal evolution of the different types of aerosols
476 that characterize the atmosphere in Northern and Southern Italy.

477 It is also worth noticing that the time series, both for all-sky conditions and for clear-sky conditions, show in some
478 seasons relevant minima in the periods 1982-1983 and 1992-1993 possibly as a consequence of the El Chichón (April
479 1982) and Pinatubo (June 1991) volcanic eruptions, which injected high amounts of sulfur dioxide into the stratosphere
480 causing a worldwide reduction in direct solar radiation (e.g., Robock, 2000; Sanchez-Lorenzo et al., 2009).

481 The observed trends under all-sky conditions are in good agreement with those observed in other worldwide areas and
482 Europe. In particular, we compared the Italian trends with those obtained by Sanchez-Lorenzo et al. (2015), using a new
483 version of the GEBA (Global Energy Balance Archive) dataset updated to 2012, for Southern Europe. This comparison
484 shows similar trends in the dimming period while in the brightening period the trends are significantly stronger for Italy
485 than for Southern Europe. This is in agreement with the SD trends reported by Manara et al. (2015) for Italy where the
486 brightening especially in the Northern region appeared to be stronger as compared to Europe.

487 The all-sky SSR trends presented for the Italian territory show some discrepancies with respect to the trends of SD
488 obtained for the same areas reported by Manara et al. (2015), despite the fact that the correlations between the two
489 variables over the period 1959-2013 are comprised between 0.71 in autumn and 0.88 in spring in the North and between
490 0.58 in autumn and 0.75 in spring in the South. The deviation of the SSR series with respect to the SD series is a trend
491 reversal shifted from the mid-1980s to the beginning of the 1980s and a dimming period that is more intense and
492 significant. The agreement between the two variables increases if the correlations between the residuals (ratio between
493 the anomaly series and the filter) are considered; they are comprised between 0.72 in summer and 0.91 in winter in the
494 North and 0.62 at annual scale and 0.84 in spring for the South highlighting a good year-to-year correlation between the
495 two variables.

496 The fact that the dimming in SD is weaker than in SSR could indicate that the long-term increase in aerosols affects the
497 two variables in a different way inducing a more significant reduction in the intensity of SSR than in SD. The
498 discrepancies between SSR and SD trends could also be a consequence of a different sensitivity to changes in the
499 diurnal cycle and decadal variability of cloud cover, temperature and humidity that could modify the measurements of
500 SD differently than SSR, but the reasons for these differences need further research. However, Sanchez-Romero et al.
501 (2014) in a review reported some studies that found similar discrepancies between SD and SSR trends in different areas
502 of the world as for example Germany (Power, 2003), China (Che et al., 2005; Zhang et al., 2004), United States
503 (Stanhill and Cohen, 2005) and Canadian Prairie (Cutforth and Judiesch, 2007).

504 A more detailed understanding of the mechanisms driving the SSR variability in Italy both under all-sky and clear-sky
505 conditions calls for further research including also the study of other variables as for example temperature, visibility,
506 aerosols and cloudiness.

507

508 **Acknowledgments**

509 We gratefully thank all the institutions that allowed access to the data for research purposes and contributed to set up
510 the 1959-2013 surface solar radiation database. They are listed below (websites and contact persons are provided for
511 data access). We received the Italian Air Force data (“Servizio dell’Aeronautica Militare Italiana”) in the frame of an
512 agreement between Italian Air Force and the Italian National Research Council (for data access refer to
513 <http://clima.meteoam.it/istruzioni.php>). In the frame of this agreement we also obtained the cloudiness data used to
514 discriminate the clear days. For the BDAN (“Banca Dati Agrometeorologica Nazionale”) data refer to
515 <http://cma.entecra.it/homePage.htm> and for Trieste observatory refer to <http://www.meteo.units.it/>. The Swiss data were
516 obtained from the Swiss Federal Office for Meteorology and Climatology (MeteoSwiss) and they are available at
517 <http://www.meteosvizzera.admin.ch/>. The Sahel Precipitation Index data came from the Joint Institute for the Study of
518 the Atmosphere and Ocean and they are available at http://research.jisao.washington.edu/data_sets/sahel/. Arturo
519 Sanchez-Lorenzo was supported by a postdoctoral fellowship JCI-2012-12508, and projects CGL2014-55976-R and
520 CGL2014-52135-C3-1-R financed by the Spanish Ministry of Economy and Competitiveness. We also kindly
521 acknowledge Ruth Loewenstein for the help in improving the English.

522

523 **References**

- 524 Aguilar, E., Auer, I., Brunet, M., Peterson, T. C. and Wieringa, J.: Guidelines on climate metadata and homogenization,
525 World Climate Programme Data and Monitoring WCDMP-No. 53, WMO-TD No. 1186, 1186, 50, 2003.
- 526 Albrecht, B. A.: Aerosols, cloud microphysics, and fractional cloudiness, *Science*, 245(4923), 1227–1230,
527 doi:10.1126/science.245.4923.1227, 1989.
- 528 Allen, R. J., Norris, J. R. and Wild, M.: Evaluation of multidecadal variability in CMIP5 surface solar radiation and

- 529 inferred underestimation of aerosol direct effects over Europe, China, Japan, and India, *Journal of Geophysical*
530 *Research: Atmospheres*, 118(12), 6311–6336, doi:10.1002/jgrd.50426, 2013.
- 531 Alpert, P., Kishcha, P., Kaufman, Y. J. and Schwarzbard, R.: Global dimming or local dimming?: Effect of urbanization
532 on sunlight availability, *Geophysical Research Letters*, 32(17), L17802, doi:10.1029/2005GL023320, 2005.
- 533 De Angelis, M. and Gaudichet, A.: Saharan dust deposition over Mont Blanc (French Alps) during the last 30 years,
534 *Tellus*, 43B, 61–75, 1991.
- 535 Bonasoni, P., Cristofanelli, P., Calzolari, F., Bonafè, U., Evangelisti, F., Stohl, A., Sajani Zauli, S., van Dingenen, R.,
536 Colombo, T. and Balkanski, Y.: Aerosol-ozone correlations during dust transport episodes, *Atmospheric Chemistry and*
537 *Physics*, 4, 1201–1215, doi:1680-7324/acp/2004-4-1201, 2004.
- 538 Brunetti, M., Maugeri, M., Nanni, T., Auer, I., Böhm, R. and Schöner, W.: Precipitation variability and changes in the
539 greater Alpine region over the 1800-2003 period, *Journal of Geophysical Research: Atmospheres*, 111(11), 1–29,
540 doi:10.1029/2005JD006674, 2006a.
- 541 Brunetti, M., Maugeri, M., Monti, F. and Nanni, T.: Temperature and precipitation variability in Italy in the last two
542 centuries from homogenised instrumental time series, *International Journal of Climatology*, 26(3), 345–381,
543 doi:10.1002/joc.1251, 2006b.
- 544 Che, H. Z., Shi, G. Y., Zhang, X. Y., Arimoto, R., Zhao, J. Q., Xu, L., Wang, B. and Chen, Z. H.: Analysis of 40 years
545 of solar radiation data from China, 1961-2000, *Geophysical Research Letters*, 32, L06803, doi:10.1029/2004GL022322,
546 2005.
- 547 Cherian, R., Quaas, J., Salzmann, M. and Wild, M.: Pollution trends over Europe constrain global aerosol forcing as
548 simulated by climate models, *Geophysical Research Letters*, 41, 2176–2181, doi:10.1002/2013GL0587151., 2014.
- 549 Chiacchio, M. and Wild, M.: Influence of NAO and clouds on long-term seasonal variations of surface solar radiation in
550 Europe, *Journal of Geophysical Research*, 115, D00D22, doi:10.1029/2009JD012182, 2010.
- 551 Craddock, J. M.: Methods of comparing annual rainfall records for climatic purposes., *Weather*, 34(9), 332–346, 1979.
- 552 Cutforth, H. W. and Judiesch, D.: Long-term changes to incoming solar energy on the Canadian Prairie, *Agricultural*
553 *and Forest Meteorology*, 145, 167–175, doi:10.1016/j.agrformet.2007.04.011, 2007.
- 554 Dutton, E. G., Stone, R. S., Nelson, D. W. and Mendonca, B. G.: Recent interannual variations in solar radiation,
555 cloudiness, and surface temperature at the South Pole, *Journal of Climate*, 4(8), 848–858, 1991.
- 556 Dutton, E. G., Farhadi, A., Stone, R. S., Long, C. N. and Nelson, D. W.: Long-term variations in the occurrence and
557 effective solar transmission of clouds as determined from surface-based total irradiance observations, *Journal of*
558 *Geophysical Research: Atmospheres*, 109(D3), doi:10.1029/2003JD003568, 2004.
- 559 Dutton, E. G., Nelson, D. W., Stone, R. S., Longenecker, D., Carbaugh, G., Harris, J. M. and Wendell, J.: Decadal
560 variations in surface solar irradiance as observed in a globally remote network, *Journal of Geophysical Research:*
561 *Atmospheres*, 111(D19), 1–10, doi:10.1029/2005JD006901, 2006.
- 562 Folini, D. and Wild, M.: Aerosol emissions and dimming/brightening in Europe: Sensitivity studies with ECHAM5-
563 HAM, *Journal of Geophysical Research: Atmospheres*, 116(D21), 1–15, doi:10.1029/2011JD016227, 2011.
- 564 Gilgen, H., Wild, M. and Ohmura, A.: Means and trends of shortwave irradiance at the surface estimated from global
565 energy balance archive data, *Journal of Climate*, 11, 2042–2061, doi:10.1175/1520-0442-11.8.2042, 1998.
- 566 Gkikas, A., Hatzianastassiou, N., Mihalopoulos, N., Katsoulis, V., Kazadzis, S., Pey, J., Querol, X. and Torres, O.: The
567 regime of intense desert dust episodes in the Mediterranean based on contemporary satellite observations and ground
568 measurements, *Atmospheric Chemistry and Physics*, 13(23), 12135–12154, doi:10.5194/acp-13-12135-2013, 2013.
- 569 Hansen, J., Sato, M. and Ruedy, R.: Radiative forcing and climate response, *Journal of Geophysical Research:*
570 *Atmospheres*, 102(D6), 6831–6864, doi:10.1029/96JD03436, 1997.
- 571 Hartmann, D. L., Ramanathan, V., Berroir, A. and Hunt, G. E.: Earth Radiation Budget Data and Climate Research,
572 *Reviews of Geophysics*, 24(2), 439–468, 1986.
- 573 Italian Air Force: La radiazione solare globale e la durata del soleggiamento in Italia dal 1991 al 2010, *Areonautica*
574 *Militare, Reparto di Sperimentazione di Meteorologica Areonautica*, 1–53, 2012.
- 575 Kvalevåg, M. M. and Myhre, G.: Human impact on direct and diffuse solar radiation during the industrial era, *Journal*
576 *of Climate*, 20, 4874–4883, doi:10.1175/JCLI4277.1, 2007.
- 577 Li, Z., Xia, X., Cribb, M., Mi, W., Holben, B., Wang, P., Chen, H., Tsay, S.-C., Eck, T. F., Zhao, F., Dutton, E. G. and
578 Dickerson, R. E.: Aerosol optical properties and their radiative effects in northern China, *Journal of Geophysical*

- 579 Research Atmospheres, 112(22), 1–11, doi:10.1029/2006JD007382, 2007.
- 580 Liang, F. and Xia, X. A.: Long-term trends in solar radiation and the associated climatic factors over China for 1961-
581 2000, *Annales Geophysicae*, 23(7), 2425–2432, doi:10.5194/angeo-23-2425-2005, 2005.
- 582 Liepert, B. and Tegen, I.: Multidecadal solar radiation trends in the United States and Germany and direct tropospheric
583 aerosol forcing, *Journal of Geophysical Research: Atmospheres*, 107(D12), AAC 7–1–AAC 7–15,
584 doi:10.1029/2001jd000760, 2002.
- 585 Liepert, B., Fabian, P. and Grassl, H.: Solar radiation in Germany - observed trends and an assessment of their causes.
586 Part I: regional approach, *Contributions to Atmospheric Physics*, 67(1), 15–29, 1994.
- 587 Liepert, B. G.: Observed reductions of surface solar radiation at sites in the United States and worldwide from 1961 to
588 1990, *Geophysical Research Letters*, 29(10), 61–1–61–4, doi:10.1029/2002GL014910, 2002.
- 589 Lohmann, U. and Feichter, J.: Global indirect aerosol effects: a review, *Atmospheric Chemistry and Physics*, 5, 715–
590 737, doi:1680-7324/acp/2005-5-715, 2005.
- 591 Long, C. N. and Ackerman, T. P.: Identification of clear skies from broadband pyranometer measurements and
592 calculation of downwelling shortwave cloud effects, *Journal of Geophysical Research*, 105(D12), 15609–15626,
593 doi:10.1029/2000JD900077, 2000.
- 594 Long, C. N., Dutton, E. G., Augustine, J. A., Wiscombe, W., Wild, M., McFarlane, S. A. and Flynn, C. J.: Significant
595 decadal brightening of downwelling shortwave in the continental United States, *Journal of Geophysical Research*, 114,
596 D00D06, doi:10.1029/2008JD011263, 2009.
- 597 Maggi, V., Villa, S., Finizio, A., Delmonte, B., Casati, P. and Marino, F.: Variability of anthropogenic and natural
598 compounds in high altitude-high accumulation alpine glaciers, *Hydrobiologia*, 562, 43–56, doi:10.1007/s10750-005-
599 1804-y, 2006.
- 600 Manara, V., Beltrano, M. C., Brunetti, M., Maugeri, M., Sanchez-Lorenzo, A., Simolo, C. and Sorrenti, S.: Sunshine
601 duration variability and trends in Italy from homogenized instrumental time series (1936-2013), *Journal of Geophysical*
602 *Research: Atmospheres*, 120(9), 3622–3641, doi:10.1002/2014JD022560, 2015.
- 603 Mateos, D., Sanchez-Lorenzo, A., Antón, M., Cachorro, V. E., Calbó, J., Costa, M. J., Torres, B. and Wild, M.:
604 Quantifying the respective roles of aerosols and clouds in the strong brightening since the early 2000s over the Iberian
605 Peninsula, *Journal of Geophysical Research: Atmospheres*, 119(17), 10382–10393, doi:10.1002/2014JD022076, 2014.
- 606 Maugeri, M., Bagnati, Z., Brunetti, M. and Nanni, T.: Trends in Italian total cloud amount, 1951-1996, *Geophysical*
607 *Research Letters*, 28(24), 4551–4554, doi:10.1029/2001GL013754, 2001.
- 608 Mylona, S.: Sulphur dioxide emissions in Europe 1880-1991 and their effect on sulphur concentrations and depositions,
609 *Tellus*, 48B, 662–689, 1996.
- 610 Nabat, P., Somot, S., Mallet, M., Sanchez-Lorenzo, A. and Wild, M.: Contribution of anthropogenic sulfate aerosols to
611 the changing Euro-Mediterranean climate since 1980, *Geophysical Research Letters*, 41(15), 5605–5611,
612 doi:10.1002/2014GL060798, 2014.
- 613 Nabat, P., Somot, S., Mallet, M., Sevault, F., Chiacchio, M. and Wild, M.: Direct and semi-direct aerosol radiative
614 effect on the Mediterranean climate variability using a coupled regional climate system model, *Climate Dynamics*,
615 44(3), 1127–1155, doi:10.1007/s00382-014-2205-6, 2015.
- 616 Norris, J. R. and Wild, M.: Trends in aerosol radiative effects over Europe inferred from observed cloud cover, solar
617 “dimming,” and solar “brightening,” *Journal of Geophysical Research*, 112(D8), D08214, doi:10.1029/2006JD007794,
618 2007.
- 619 Novakov, T., Ramanathan, V., Hansen, J. E., Kirchstetter, T. W., Sato, M., Sinton, J. E. and Sathaye, J. A.: Large
620 historical changes of fossil-fuel black carbon aerosols, *Geophysical Research Letters*, 30(6), 1324,
621 doi:10.1029/2002GL016345, 2003.
- 622 Ohmura, A.: Observed decadal variations in surface solar radiation and their causes, *Journal of Geophysical Research*,
623 114(D10), D00D05, doi:10.1029/2008JD011290, 2009.
- 624 Ohmura, A. and Lang, H.: Secular variation of global radiation in Europe, IRS’88: Current Problems In Atmospheric
625 Radiation, Lenoble, J. and Geleyn, J.-F. (Eds). A. Deepak Publ., Hampton, VA., 98–301, 1989.
- 626 Parding, K., Olseth, J. A., Dagestad, K. F. and Liepert, B. G.: Decadal variability of clouds, solar radiation and
627 temperature at a high-latitude coastal site in Norway, *Tellus B*, 66, doi:10.3402/tellusb.v66.25897, 2014.
- 628 Pey, J., Querol, X., Alastuey, A., Forastiere, F. and Stafoggia, M.: African dust outbreaks over the Mediterranean Basin
629 during 2001-2011: PM10 concentrations, phenomenology and trends, and its relation with synoptic and mesoscale

- 630 meteorology, *Atmospheric Chemistry and Physics*, 13(3), 1395–1410, doi:10.5194/acp-13-1395-2013, 2013.
- 631 Power, H. C.: Trends in solar radiation over Germany and an assessment of the role of aerosols and sunshine duration,
632 *Theoretical and Applied Climatology*, 76, 47–63, doi:10.1007/s00704-003-0005-8, 2003.
- 633 Preisendorfer, R. W.: *Principal component analysis in meteorology and oceanography*, edited by Elsevier, New York.,
634 1988.
- 635 Prospero, J. M.: Saharan dust transport over the North Atlantic Ocean and Mediterranean: An overview, *The Impact of*
636 *Desert Dust across the Mediterranean*, 11, 133–151, doi:10.1007/978-94-017-3354-0, 1996.
- 637 Radke, L. F., Coakley, J. A. and King, M. D.: Direct and remote sensing observations of the effects of ships on clouds.,
638 *Science*, 246(4934), 1146–1149, doi:10.1126/science.246.4934.1146, 1989.
- 639 Ramanathan, V., Crutzen, P. J., Kiehl, J. T. and Rosenfeld, D.: Aerosols, Climate, and the Hydrological Cycle, *Science*,
640 294(5549), 2119–2124, doi:10.1126/science.1064034, 2001.
- 641 Robock, A.: Volcanic eruptions and climate, *Reviews of Geophysics*, 38(2), 191–219, doi:doi:10.1029/1998RG000054,
642 2000.
- 643 Romanou, A., Liepert, B., Schmidt, G. A., Rossow, W. B., Ruedy, R. A. and Zhang, Y.: 20th Century Changes in
644 Surface Solar Irradiance in Simulations and Observations, *Geophysical Research Letters*, 34(5),
645 doi:10.1029/2006GL028356, 2007.
- 646 Ruckstuhl, C. and Norris, J. R.: How do aerosol histories affect solar “dimming” and “brightening” over Europe?:
647 IPCC-AR4 models versus observations, *Journal of Geophysical Research*, 114, D00D04, doi:10.1029/2008JD011066,
648 2009.
- 649 Ruckstuhl, C., Philipona, R., Behrens, K., Collaud Coen, M., Dürr, B., Heimo, A., Mätzler, C., Nyeki, S., Ohmura, A.,
650 Vuilleumier, L., Weller, M., Wehrli, C. and Zelenka, A.: Aerosol and cloud effects on solar brightening and the recent
651 rapid warming, *Geophysical Research Letters*, 35(12), doi:10.1029/2008GL034228, 2008.
- 652 Russak, V.: Trends of solar radiation, cloudiness and atmospheric transparency during recent decades in Estonia, *Tellus*,
653 *Series B*, 42 B(2), 206–210, 1990.
- 654 Sanchez-Lorenzo, A. and Wild, M.: Decadal variations in estimated surface solar radiation over Switzerland since the
655 late 19th century, *Atmospheric Chemistry and Physics*, 12(18), 8635–8644, doi:10.5194/acp-12-8635-2012, 2012.
- 656 Sanchez-Lorenzo, A., Calbó, J., Brunetti, M. and Deser, C.: Dimming/brightening over the Iberian Peninsula: Trends in
657 sunshine duration and cloud cover and their relations with atmospheric circulation, *Journal of Geophysical Research*,
658 114, D00D09, doi:10.1029/2008JD011394, 2009.
- 659 Sanchez-Lorenzo, A., Calbó, J. and Wild, M.: Global and diffuse solar radiation in Spain: Building a homogeneous
660 dataset and assessing their trends, *Global and Planetary Change*, 100, 343–352, doi:10.1016/j.gloplacha.2012.11.010,
661 2013.
- 662 Sanchez-Lorenzo, A., Wild, M., Brunetti, M., Guijarro, J. A., Hakuba, M. Z., Calbó, J., Mystakidis, S. and Bartok, B.:
663 Reassessment and update of long-term trends in downward surface shortwave radiation over Europe (1939-2012),
664 *Journal of Geophysical Research: Atmospheres*, 120(18), 9555–9569, doi:10.1002/2015JD023321, 2015.
- 665 Sanchez-Romero, A., Sanchez-Lorenzo, A., Calbó, J., González, J. A. and Azorin-Molina, C.: The signal of aerosol-
666 induced changes in sunshine duration records: A review of the evidence, *Journal of Geophysical Research:*
667 *Atmospheres*, 119(8), 4657–4673, doi:10.1002/2013JD021393, 2014.
- 668 Sanchez-Romero, A., Sanchez-Lorenzo, A., González, J. A. and Calbó, J.: Reconstruction of long-term aerosol optical
669 depth series with sunshine duration records, *Geophysical Research Letters*, 43, doi:10.1002/2015GL067543, 2016.
- 670 Sneyers, R.: On the use of statistical analysis for the objective determination of climate change, *Meteorologische*
671 *Zeitschrift*, 1(5), 247–256, 1992.
- 672 Spinoni, J., Brunetti, M., Maugeri, M. and Simolo, C.: 1961–1990 monthly high-resolution solar radiation climatologies
673 for Italy, *Advances in Science and Research*, 8, 19–25, doi:10.5194/asr-8-19-2012, 2012.
- 674 Stanhill, G.: The distribution of global solar radiation over the land surfaces of the Earth, *Solar Energy*, 31(1), 95–104,
675 1983.
- 676 Stanhill, G. and Cohen, S.: Global dimming: A review of the evidence for a widespread and significant reduction in
677 global radiation with discussion of its probable causes and possible agricultural consequences, *Agricultural and Forest*
678 *Meteorology*, 107(4), 255–278, doi:10.1016/S0168-1923(00)00241-0, 2001.
- 679 Stanhill, G. and Cohen, S.: *Solar Radiation Changes in the United States during the Twentieth Century : Evidence from*

- 680 Sunshine Duration Measurements, American Meteorological Society, 18(10), 1503–1512, 2005.
- 681 Stanhill, G. and Moreshet, S.: Global radiation climate changes: The world network, *Climatic Change*, 21(1), 57–75,
682 doi:10.1007/BF00143253, 1992.
- 683 Von Storch, H.: Spatial Patterns: EOFs and CCA, in *Analysis of Climate Variability: Applications of Statistical*
684 *Techniques*, edited by A. Navarra and H. von Storch, Application of Statistical Techniques, 227–258, 1995.
- 685 Stravisi, F.: TRIESTE Dati orari di irradianza solare 1971-2003, Università degli Studi di Trieste-Dipartimento di
686 Scienze della Terra Rapporti OM N. 105, 2004.
- 687 Stravisi, F. and Cirilli, S.: Irradianza solare globale 2013, Università degli Studi di Trieste-Dipartimento di Scienze
688 della Terra, Rap n° 159, 2014.
- 689 Streets, D. G., Wu, Y. and Chin, M.: Two-decadal aerosol trends as a likely explanation of the global
690 dimming/brightening transition, *Geophysical Research Letters*, 33(15), L15806, doi:10.1029/2006GL026471, 2006.
- 691 Streets, D. G., Yan, F., Chin, M., Diehl, T., Mahowald, N., Schultz, M., Wild, M., Wu, Y. and Yu, C.: Anthropogenic
692 and natural contributions to regional trends in aerosol optical depth, 1980-2006, *Journal of Geophysical Research*,
693 114(D10), 1–16, doi:10.1029/2008JD011624, 2009.
- 694 Turnock, S. T., Spracklen, D. V., Carslaw, K. S., Mann, G. W., Woodhouse, M. T., Forster, P. M., Haywood, J.,
695 Johnson, C. E., Dalvi, M., Bellouin, N. and Sanchez-Lorenzo, A.: Modelled and observed changes in aerosols and
696 surface solar radiation over Europe between 1960 and 2009, *Atmospheric Chemistry and Physics*, 15(16), 9477–9500,
697 doi:10.5194/acp-15-9477-2015, 2015.
- 698 Twomey, S. A., Piepgrass, M. and Wolfe, T. L.: An assessment of the impact of pollution on global cloud albedo,
699 *Tellus*, 36B, 356–366, doi:10.1111/j.1600-0889.1984.tb00254.x, 1984.
- 700 USGS: GTOPO 30 Digital Elevation Model, [online] Available from: <https://lta.cr.usgs.gov/GTOPO30>, 1996.
- 701 Varga, G., Újvári, G. and Kovács, J.: Spatiotemporal patterns of Saharan dust outbreaks in the Mediterranean Basin,
702 *Aeolian Research*, 15, 151–160, doi:10.1016/j.aeolia.2014.06.005, 2014.
- 703 Vestreng, V., Myhre, G., Fagerli, H., Reis, S. and Tarrasón, L.: Twenty-five years of continuous sulphur dioxide
704 emission reduction in Europe, *Atmospheric Chemistry and Physics*, 7(13), 3663–3681, doi:10.5194/acp-7-3663-2007,
705 2007.
- 706 Wang, K. C., Dickinson, R. E., Wild, M. and Liang, S.: Atmospheric impacts on climatic variability of surface incident
707 solar radiation, *Atmospheric Chemistry and Physics*, 12(20), 9581–9592, doi:10.5194/acp-12-9581-2012, 2012.
- 708 Wang, Y. W. and Yang, Y. H.: China's dimming and brightening: evidence, causes and hydrological implications,
709 *Annales Geophysicae*, 32, 41–55, doi:10.5194/angeo-32-41-2014, 2014.
- 710 Wild, M.: Global dimming and brightening: A review, *Journal of Geophysical Research*, 114, D00D16,
711 doi:10.1029/2008JD011470, 2009.
- 712 Wild, M.: Enlightening Global Dimming and Brightening, *Bulletin of the American Meteorological Society*, 93, 27–37,
713 doi:10.1175/BAMS-D-11-00074.1, 2012.
- 714 Wild, M.: Decadal changes in radiative fluxes at land and ocean surfaces and their relevance for global warming, *Wiley*
715 *Interdisciplinary Reviews: Climate Change*, doi:10.1002/wcc.372, 2015.
- 716 Wild, M., Gilgen, H., Roesch, A., Ohmura, A., Long, C. N., Dutton, E. G., Forgan, B., Kallis, A., Russak, V. and
717 Tsvetkov, A.: From Dimming to Brightening: Decadal Changes in Solar Radiation at Earth's Surface, *Science*,
718 308(5723), 847–850, doi:10.1126/science.1103215, 2005.
- 719 Wild, M., Trüssel, B., Ohmura, A., Long, C. N., König-Langlo, G., Dutton, E. G. and Tsvetkov, A.: Global dimming
720 and brightening: An update beyond 2000, *Journal of Geophysical Research*, 114, D00D13, doi:10.1029/2008JD011382,
721 2009.
- 722 Wilks, D. S.: Statistical methods in the atmospheric sciences, *International Geophysics Series*, 59, 464,
723 doi:10.1007/s13398-014-0173-7.2, 1995.
- 724 Xia, X.: A closer looking at dimming and brightening in China during 1961-2005, *Annales Geophysicae*, 28(5), 1121–
725 1132, doi:10.5194/angeo-28-1121-2010, 2010a.
- 726 Xia, X.: Spatiotemporal changes in sunshine duration and cloud amount as well as their relationship in China during
727 1954-2005, *Journal of Geophysical Research Atmospheres*, 115(7), 1–13, doi:10.1029/2009JD012879, 2010b.
- 728 Zhang, X., Xia, X. and Xuan, C.: On the drivers of variability and trend of surface solar radiation in Beijing
729 metropolitan area, *International Journal of Climatology*, 35(3), 452–461, doi:10.1002/joc.3994, 2015.

- 730 Zhang, Y. L., Qin, B. Q. and Chen, W. M.: Analysis of 40 year records of solar radiation data in Shanghai, Nanjing and
731 Hangzhou in Eastern China, *Theoretical and Applied Climatology*, 78, 217–227, doi:10.1007/s00704-003-0030-7,
732 2004.
- 733 Zhu, A., Ramanathan, V., Li, F. and Kim, D.: Dust plumes over the Pacific, Indian, and Atlantic oceans: Climatology
734 and radiative impact, *Journal of Geophysical Research: Atmospheres*, 112(16), 1–20, doi:10.1029/2007JD008427,
735 2007.
- 736

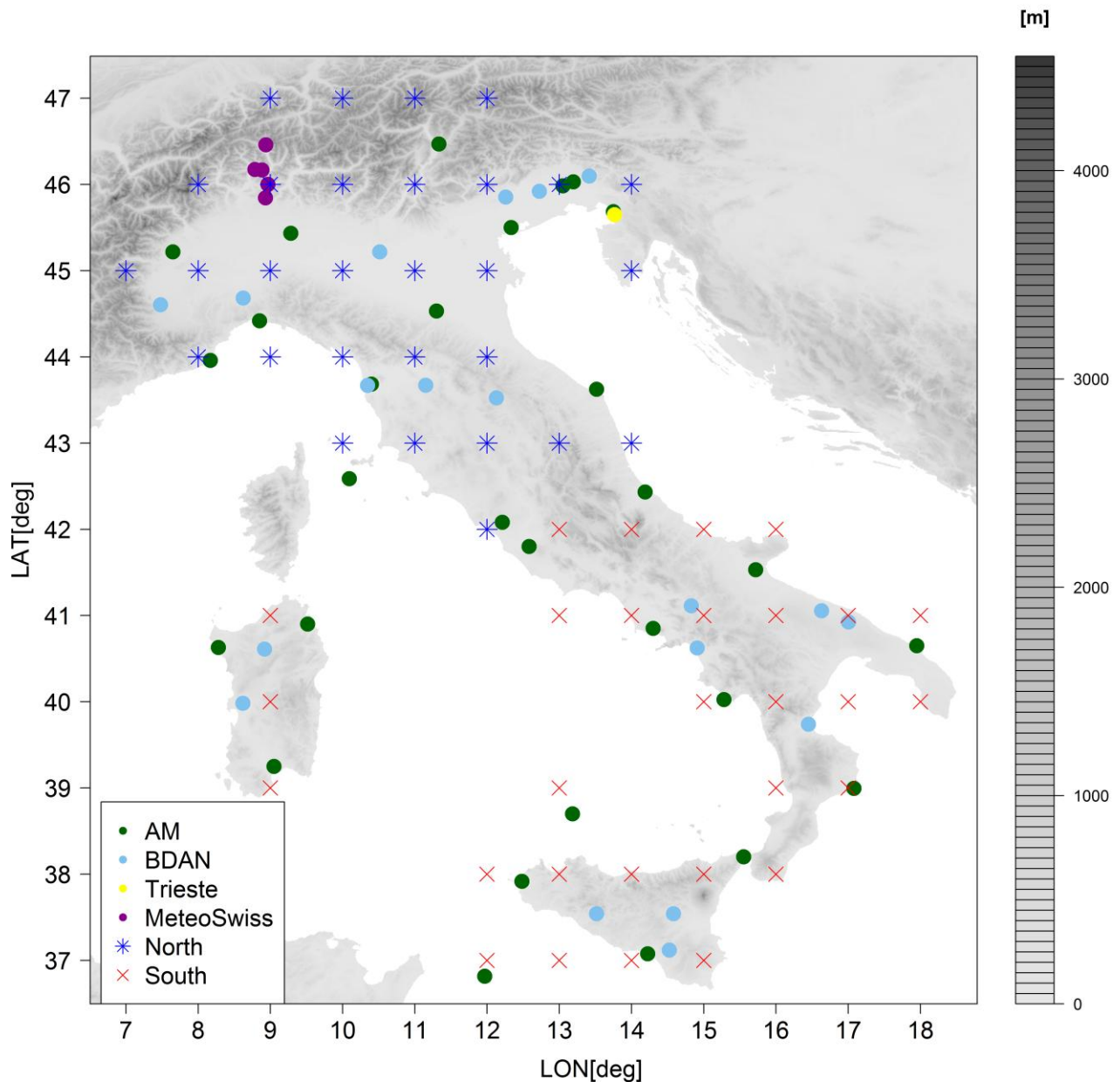
737 Table 1. Details on the network, station location, instruments and length of the records in the SSR data set. The last
738 column shows which records have been considered to calculate the regional mean under clear-sky conditions (see Sect.
739 2.4).

Network / Data Source	Station name	Country	Region	Latitude (deg)	Longitude (deg)	Elevation (m)	Period	Instrument (pyranograph, pyranometer)	Selected clear-sky 0 okta
METEO SWISS	ACQUAROSSA	CH	N	46.459	8.936	575	1988-2013	CM21 Kipp & Zonen	N
	COMPROVASCO								
AM	ALGHERO	I	S	40.630	8.280	23	1959-1989	Robitzsch	N
AM	AMENDOLA	I	S	41.530	15.720	57	1959-2010	Robitzsch and CM11 Kipp & Zonen	Y
AM	ANCONA	I	N	43.623	13.516	104	1959-1978	Robitzsch	Y
AM	CAPPUCCINI								
AM	BOLOGNA	I	N	44.530	11.300	36	1959-1989	Robitzsch	Y
AM	BOLZANO	I	N	46.467	11.333	241	1959-1988	Robitzsch	Y
AM	BRINDISI	I	S	40.650	17.950	15	1959-2013	Robitzsch and CM11 Kipp & Zonen	Y
AM	CAGLIARI ELMAS	I	S	39.250	9.050	4	1959-2013	Robitzsch and CM11 Kipp & Zonen	N
AM	CAPO MELE	I	N	43.958	8.170	220	1964-2003	Robitzsch and CM11 Kipp & Zonen	Y
AM	CAPO PALINURO	I	S	40.025	15.280	184	1959-2013	Robitzsch and CM11 Kipp & Zonen	Y
UCEA-BDAN	CARPENETO	I	N	44.681	8.624	230	1994-2013	CM11 Kipp & Zonen	Y
UCEA-BDAN	CHILIVANI	I	S	40.610	8.919	216	1994-2013	CM11 Kipp & Zonen	N
UCEA-BDAN	CIVIDALE	I	N	46.096	13.414	130	1997-2013	CM11 Kipp & Zonen	Y
AM	CROTONE	I	S	38.996	17.080	155	1959-1989	Robitzsch	Y
UCEA-BDAN	FIUME VENETO	I	N	45.920	12.724	19	1996-2013	CM11 Kipp & Zonen	Y
AM	GELA	I	S	37.076	14.225	33	1965-1997	Robitzsch and CM11 Kipp & Zonen	Y
AM	GENOVA SESTRI	I	N	44.417	8.850	2	1959-1989	Robitzsch	Y
UCEA-BDAN	LIBERTINIA	I	S	37.541	14.581	188	1994-2013	CM11 Kipp & Zonen	N
METEO SWISS	LOCARNO MONTI	CH	N	46.172	8.787	383	1981-2013	CM21 Kipp & Zonen	N
METEO SWISS	LUGANO	CH	N	46.000	8.967	273	1981-2013	CM21 Kipp & Zonen	Y
METEO SWISS	MAGADINO	CH	N	46.167	8.883	197	1981-2013	CM21 Kipp & Zonen	Y
	CADENAZZO								
AM	MESSINA	I	S	38.201	15.553	59	1959-2006	Robitzsch and CM11 Kipp & Zonen	Y
AM	MILANO LINATE	I	N	45.433	9.283	107	1959-2010	Robitzsch and CM11 Kipp & Zonen	Y
AM	NAPOLI	I	S	40.850	14.300	88	1959-1989	Robitzsch	Y
AM	OLBIA	I	S	40.900	9.517	13	1959-1988	Robitzsch	Y
UCEA-BDAN	PALO DEL COLLE	I	S	41.055	16.632	191	1994-2013	EP07 Middleton Instrument	Y
AM	PANTELLERIA ISOLA	I	S	36.817	11.967	191	1959-2009	Robitzsch and CM11 Kipp & Zonen	N
AM	PESCARA	I	S	42.433	14.189	10	1959-1987	Robitzsch	Y
UCEA-BDAN	PIANO CAPPELLE	I	S	41.113	14.827	152	1994-2013	CM11 Kipp & Zonen	Y
AM	PIANOSA ISOLA	I	N	42.586	10.094	27	1959-1979	Robitzsch	Y
UCEA-BDAN	PIETRANERA	I	S	37.541	13.517	158	1994-2013	CM11 Kipp & Zonen	Y
AM	PISA SAN GIUSTO	I	N	43.683	10.400	2	1959-2013	Robitzsch and CM11 Kipp & Zonen	Y
UCEA-BDAN	PIUBEGA	I	N	45.217	10.514	38	1997-2013	CM11 Kipp & Zonen	Y
UCEA-BDAN	PONTECAGNANO	I	S	40.623	14.911	38	1997-2013	CM11 Kipp & Zonen	Y
AM	ROMA CIAMPINO	I	S	41.800	12.583	129	1959-2009	Robitzsch and CM11 Kipp & Zonen	Y
UCEA-BDAN	SAN CASCIANO	I	N	43.670	11.151	230	1994-2013	CM11 Kipp & Zonen	Y
UCEA-BDAN	SAN PIERO A GRADO	I	N	43.668	10.346	3	1994-2013	CM11 Kipp & Zonen	Y
UCEA-BDAN	SANTA FISTA	I	N	43.523	12.130	311	1994-2013	CM11 Kipp & Zonen	Y
UCEA-BDAN	SANTA LUCIA	I	S	39.982	8.620	14	1994-2013	CM11 Kipp & Zonen	N
UCEA-BDAN	SANTO PIETRO	I	S	37.120	14.525	313	1994-2013	CM11 Kipp & Zonen	Y
UCEA-BDAN	SIBARI	I	S	39.738	16.449	10	1994-2013	CM11 Kipp & Zonen	Y
METEO SWISS	STABIO	CH	N	45.843	8.932	353	1981-2013	CM21 Kipp & Zonen	Y
UCEA-BDAN	SUSEGANA	I	N	45.853	12.258	67	1994-2013	EP07 Middleton Instrument	Y
AM	TORINO CASELLE	I	N	45.217	7.650	301	1959-1985	Robitzsch	Y
AM	TRAPANI BIRGI	I	S	37.917	12.483	7	1959-1996	Robitzsch and CM11 Kipp & Zonen	N
AM	TRIESTE	I	N	45.683	13.750	4	1959-2001	Robitzsch and CM11 Kipp & Zonen	Y
Observatory of Trieste	TRIESTE HORTIS	I	N	45.648	13.766	35	1971-2013	Robitzsch and CM Kipp & Zonen	Y
UCEA-BDAN	TURI	I	S	40.924	17.005	230	1994-2013	EP07 Middleton Instrument	N
AM	UDINE	I	N	46.029	13.196	94	1959-1978	Robitzsch	Y
AM	CAMPOFORMIDO	I	N	45.983	13.050	51	1964-2010	Robitzsch and CM11 Kipp & Zonen	Y
AM	USTICA ISOLA	I	S	38.700	13.183	250	1959-1997	Robitzsch and CM11 Kipp & Zonen	Y
AM	VENEZIA TESSERA	I	N	45.500	12.333	2	1959-1989	Robitzsch	Y
UCEA-BDAN	VERZUOLO	I	N	44.603	7.480	420	1995-2013	CM11 Kipp & Zonen	Y
AM	VIGNA DI VALLE	I	N	42.081	12.211	275	1959-2013	Robitzsch and CM11 Kipp & Zonen	Y

741 Table 2. Absolute SSR trends in Northern and Southern Italy under all-sky conditions and estimated trends assuming no
742 changes in cloudiness (see Sect. 3.3). The results concerning the dimming and brightening periods according to the
743 Northern and Southern Italy annual records are highlighted in grey^a.

	Year	Winter	Spring	Summer	Autumn	
North All-sky	1959-2013	+	+	+	3.1±0.8	-1.5±0.7
	1959-1985	-4.4±0.8	-3.0±1.3	-7.2±2.2	-3.9±1.6	-3.5±1.9
	1986-2013	7.7±1.1	3.2±1.3	10.4±2.9	12.3±1.9	4.8±1.9
	1970-2013	2.9±0.7	1.4±0.7	4.8±1.5	6.1±1.0	-
	1970-1985	-4.0±1.9	-	-	+	-7.8±4.6
	1981-2000	+	+	+	+	-
	1981-2013	6.1±0.9	2.2±1.0	9.4±2.2	9.8±1.5	+
South All-Sky	1959-2013	-	-	+	+	-2.2±0.5
	1959-1985	-6.4±1.1	-4.6±1.4	-8.5±2.3	-8.1±2.0	-4.2±1.3
	1986-2013	6.0±1.2	+	7.6±2.0	13.5±2.3	+
	1970-2013	2.1±0.7	+	3.7±1.2	5.2±1.3	-1.5±0.8
	1970-1985	-5.9±2.6	-	-	-	-7.4±3.0
	1981-2000	5.0±1.9	6.5±2.6	+	9.3±3.5	-2.4±1.7
	1981-2013	5.4±0.9	+	6.9±1.7	11.6±1.8	+
North Clear-Sky Estimated	1959-2013	+	-	+	+	-
	1959-1985	-6.3±0.8	-3.2±0.8	-5.8±2.7	-8.2±1.6	-6.0±1.3
	1986-2013	7.6±0.9	3.6±0.7	9.7±1.6	10.0±1.5	6.5±1.3
	1970-2013	2.7±0.7	0.9±0.4	2.8±1.2	5.1±0.9	1.8±0.8
	1970-1985	-5.7±1.5	-	-	-6.9±2.4	-7.5±2.7
	1981-2000	5.3±1.6	3.2±1.4	+	7.1±2.1	5.3±2.3
	1981-2013	6.4±0.7	2.7±0.6	8.0±1.2	9.3±1.1	5.5±1.0
South Clear-Sky Estimated	1959-2013	-	-	+	+	-1.9±0.6
	1959-1985	-8.4±1.0	-4.4±1.2	-10.3±2.5	-10.7±1.8	-9.1±1.1
	1986-2013	7.9±1.0	3.9±1.3	10.2±1.6	11.4±1.9	5.4±1.1
	1970-2013	2.8±0.7	1.5±0.7	4.2±1.2	4.3±1.2	+
	1970-1985	-8.1±1.8	-	-11.3±5.2	-11.8±3.3	-10.2±2.1
	1981-2000	6.4±1.5	7.2±2.3	7.7±2.4	10.7±2.5	+
	1981-2013	7.1±0.8	3.7±1.0	9.2±1.2	10.7±1.5	4.5±0.8

^aValues are expressed in Wm⁻² per decade. Values are shown for significance level 0.05 < p <= 0.1 with a thin character and for significance p <= 0.05 with a bold character. For not significant trends, only the sign of the slope is given.



745

746

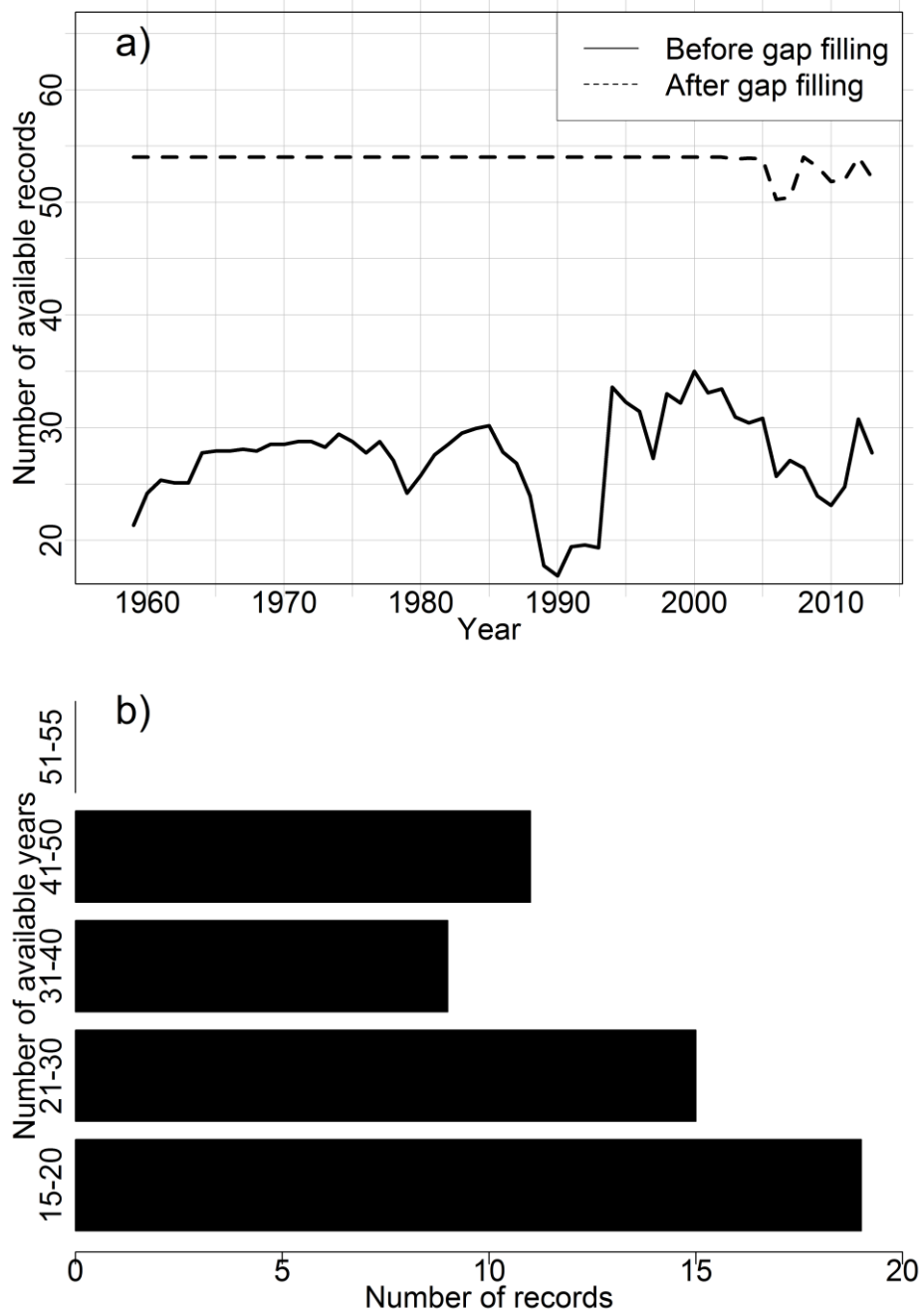
747

748

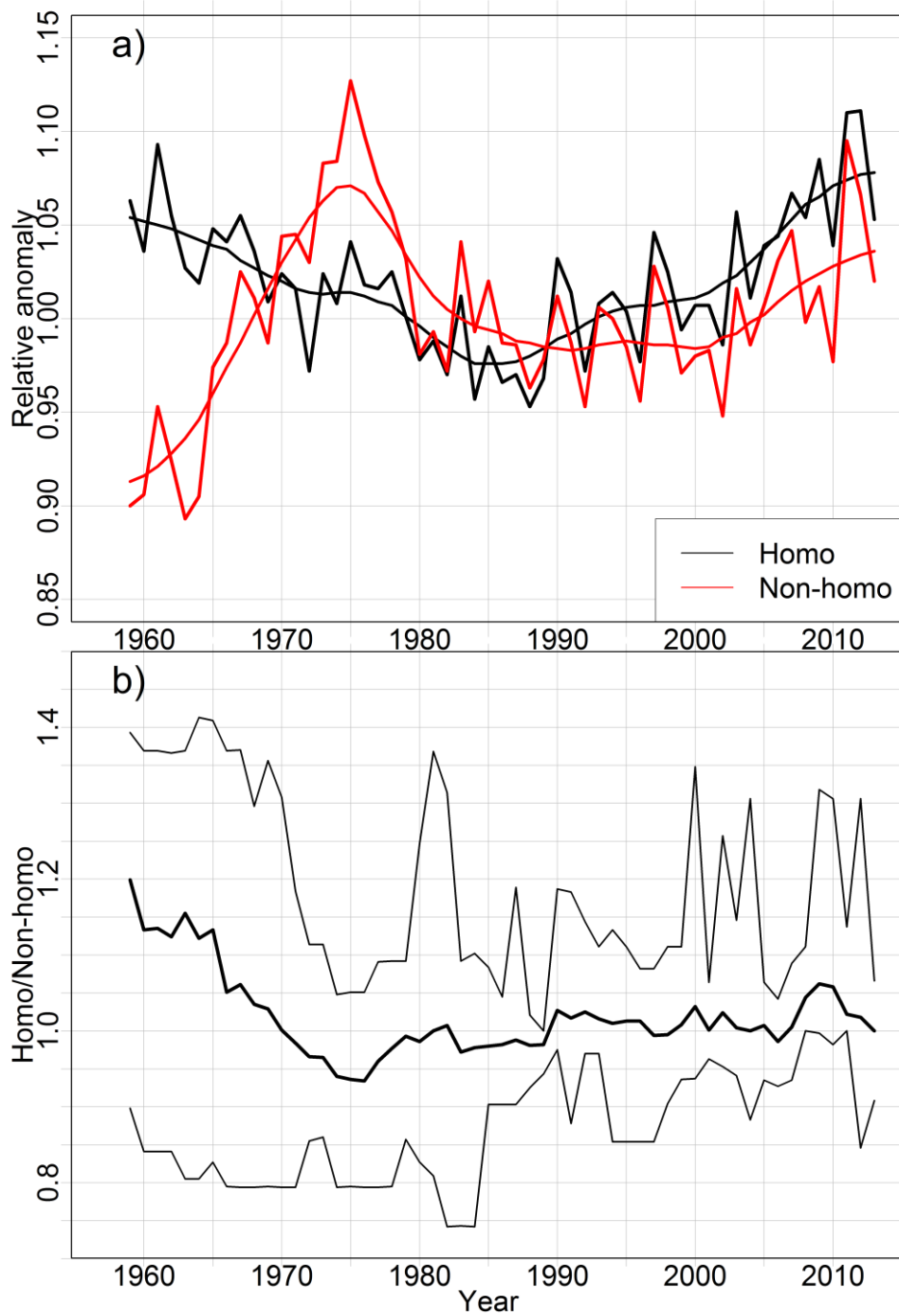
749

750

Fig. 1. Spatial distribution of the stations and of the grid-mode version of the data set (see Sect. 2.3): stars and crosses represent, respectively, Northern (29 points) and Southern (29 points) Italy grid points as clustered by a Principal Component Analysis. The figure also shows the orography of the region and gives evidence of the sources of the station records, with green circles for AM series (29 series), blue circles for BDAN series (19 series), yellow circle for the Trieste observatory and violet circles for MeteoSwiss series (5 series).

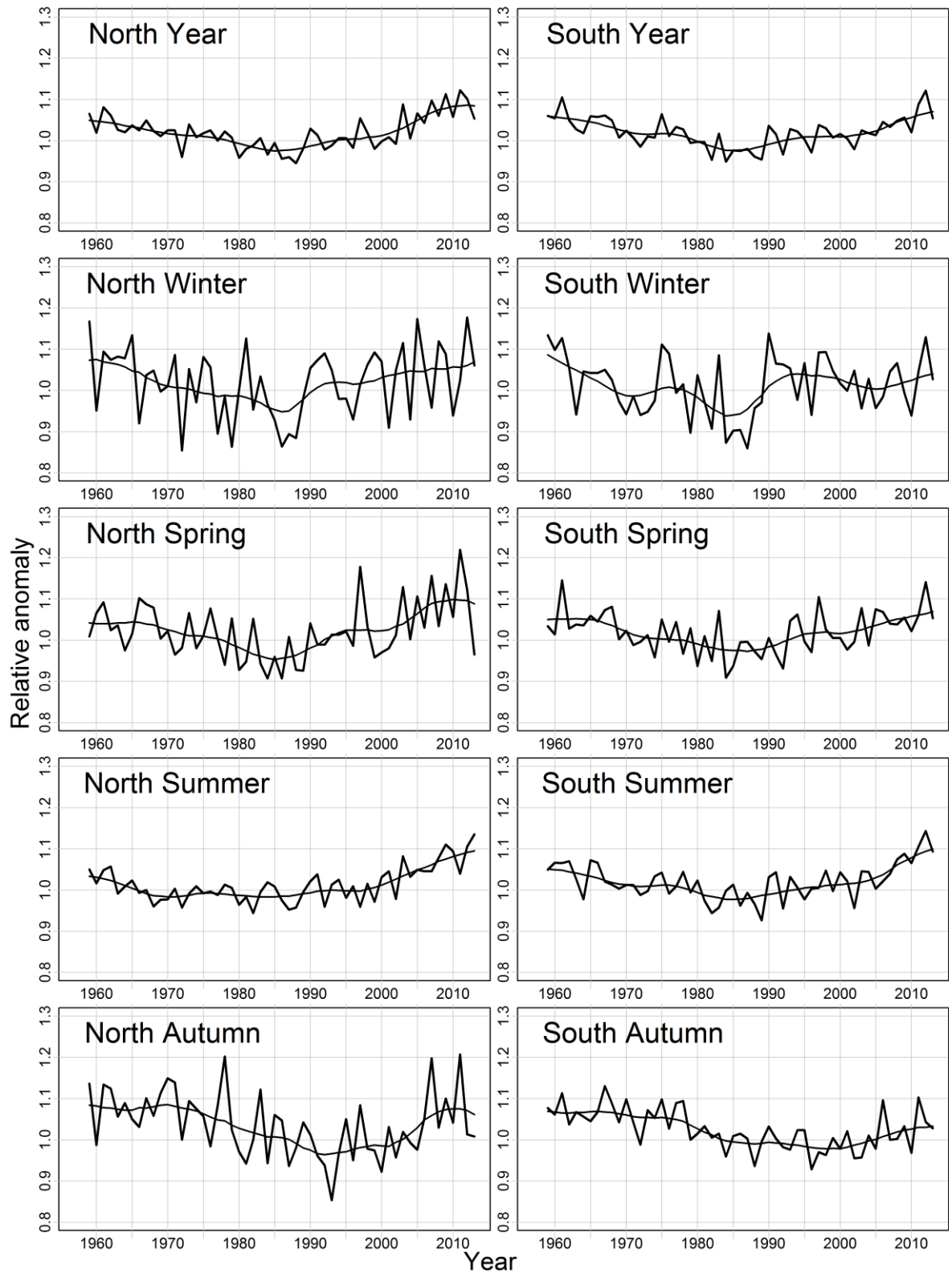


751
 752 Fig. 2. (a) Temporal evolution of the number of available records per year before (bold line) and after the gap-filling
 753 procedure (dashed line) (see Sect. 2.2); (b) The histogram shows the number of records as a function of the number of
 754 available years before the gap-filling procedure.



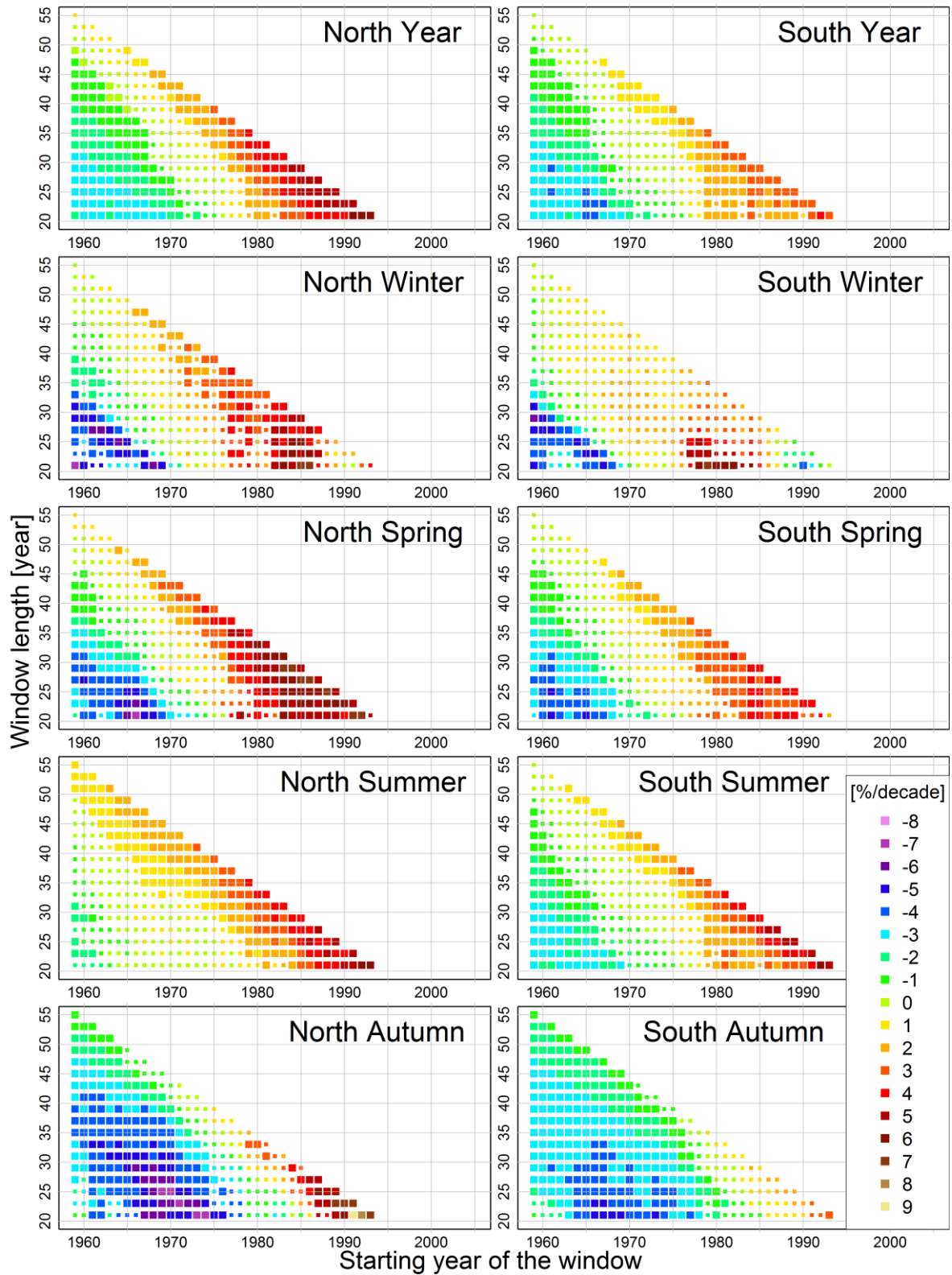
755

756 Fig. 3. (a) Average annual Italian SSR series plotted together with an 11 year window – 3-year standard deviation
 757 Gaussian low-pass filter before (red line) and after (black line) the homogenization procedure; (b) Mean annual
 758 adjustment series obtained calculating the annual average adjustment over all series (bold line). The figure shows the
 759 maximum range in the adjustments too.



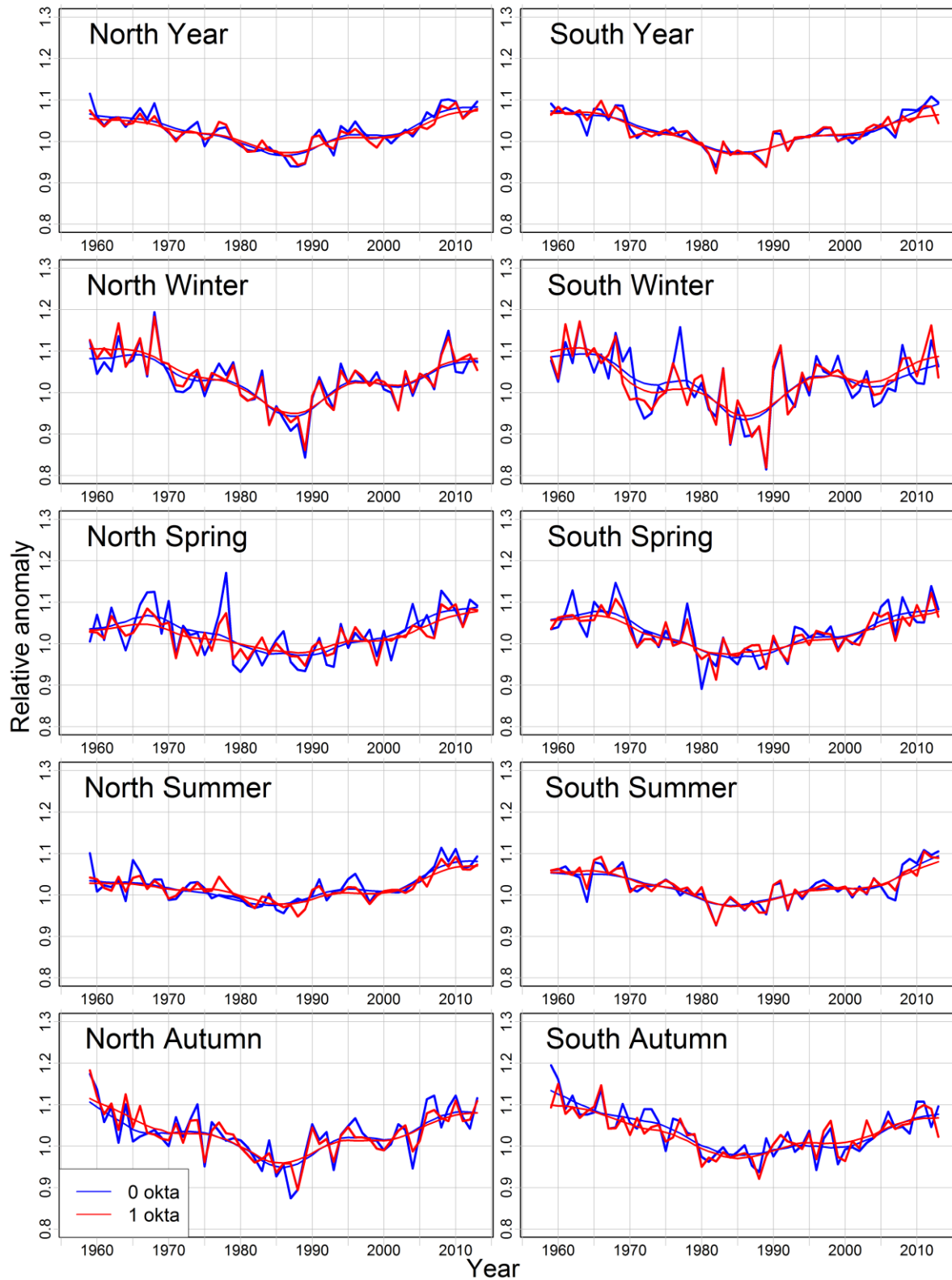
760

761 Fig. 4. Average annual and seasonal Northern (left column) and Southern (right column) Italy SSR records obtained
 762 under all-sky conditions (bold lines), plotted together with an 11 year window – 3-year standard deviation Gaussian
 763 low-pass filter (thin lines). The series are expressed as relative deviations from the 1976-2005 means.



764

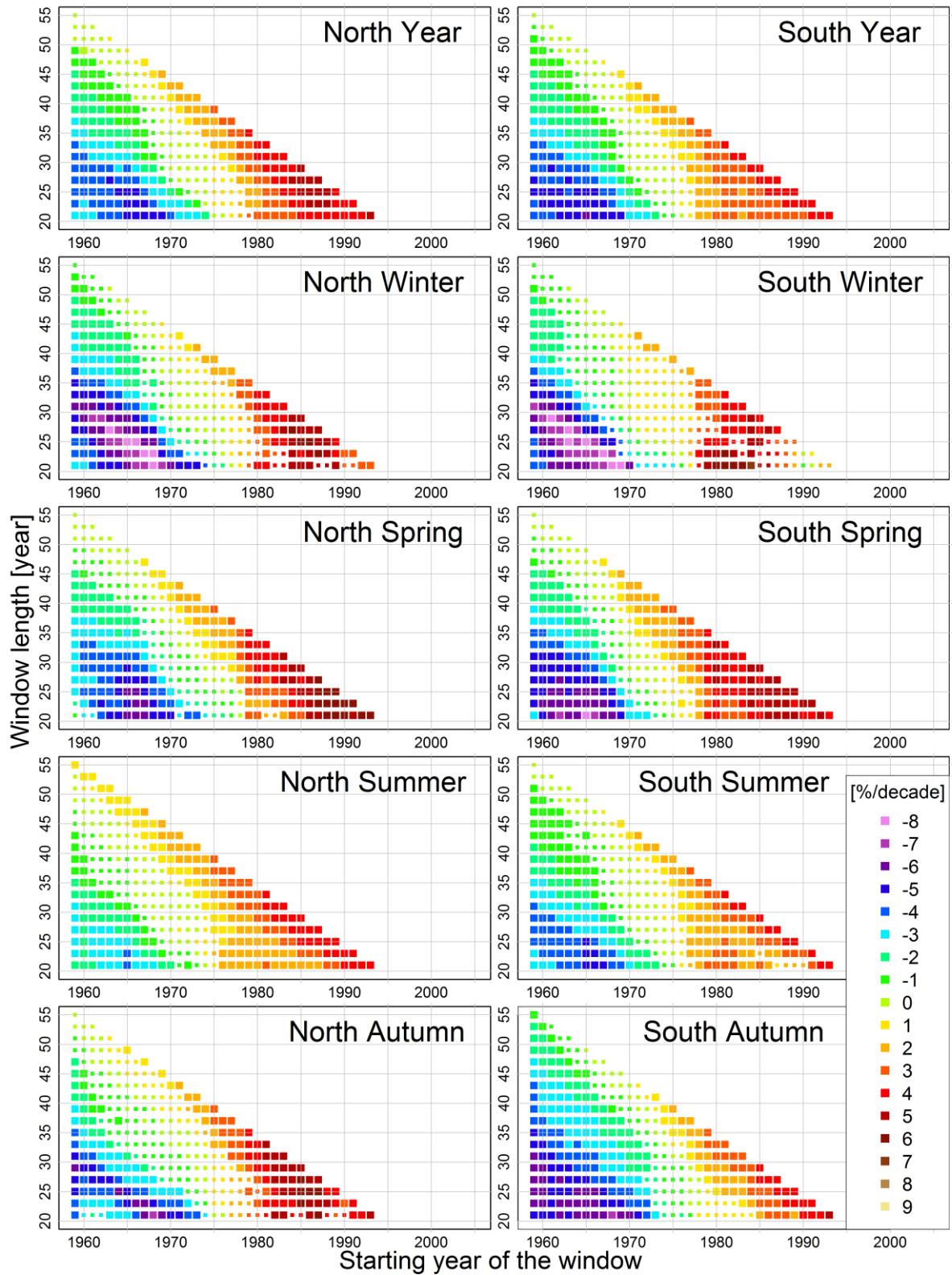
765 Fig. 5. Running trend analysis for annual and seasonal Northern (left column) and Southern (right column) Italy SSR
 766 records obtained under all-sky conditions. The y and x axis represent the length and the first year of the period under
 767 analysis, respectively, while the colored pixels show the trend expressed in %/decade with a significance level
 768 $p \leq 0.1$ (large squares) and $p > 0.1$ (small squares).
 769



770

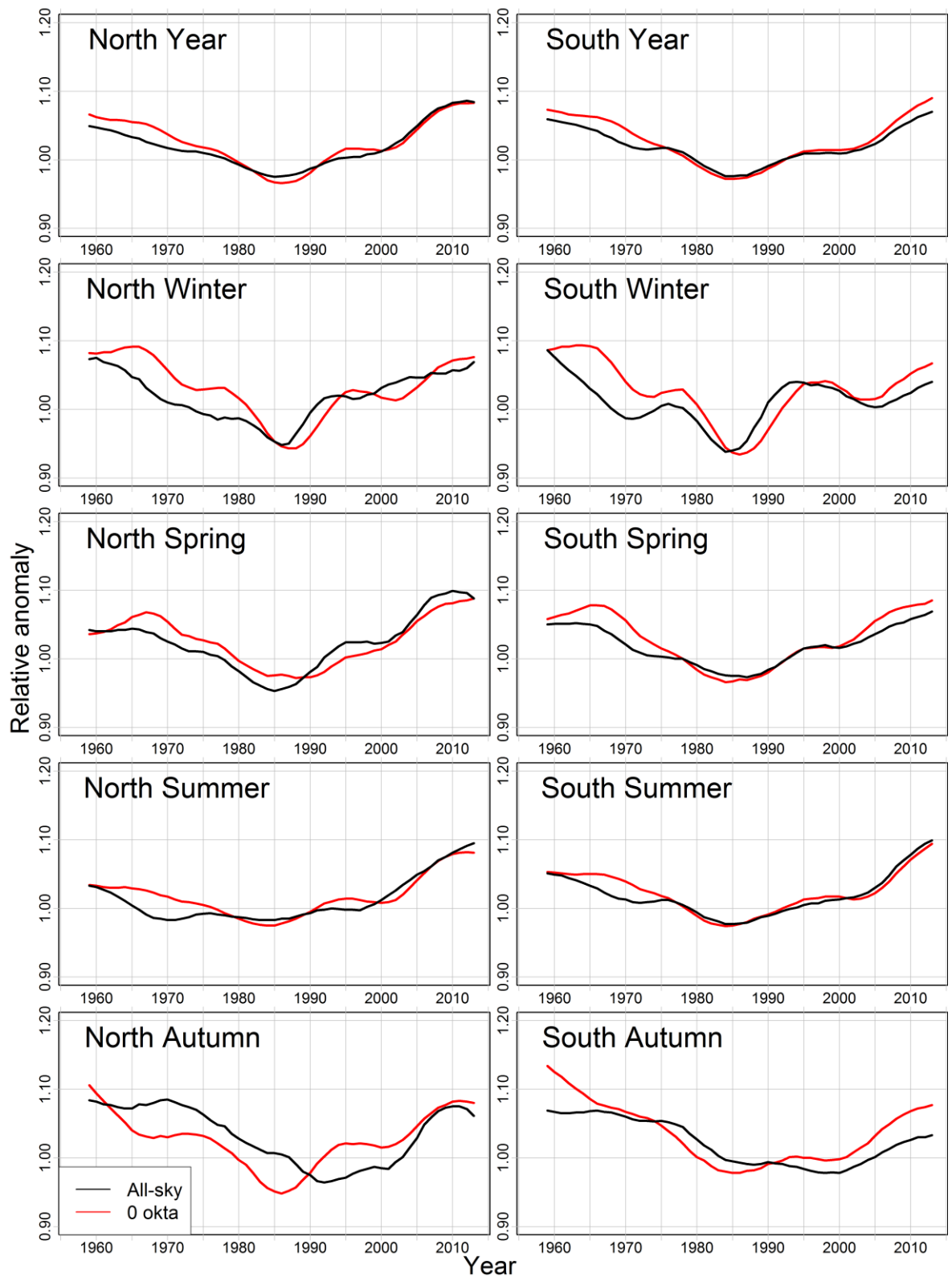
771 Fig. 6. Average annual and seasonal Northern (left column) and Southern (right column) Italy SSR records obtained
 772 under clear-sky conditions (bold lines), plotted together with an 11 year window – 3-year standard deviation Gaussian
 773 low-pass filter (thin lines). The series are expressed as relative deviations from the 1976-2005 means. The blue lines
 774 represent the records obtained using 0 okta of TCC as threshold to select clear days and the red lines the ones using 1
 775 okta.

776



777

778 Fig. 7. Running trend analysis for annual and seasonal Northern (left column) and Southern (right column) Italy SSR
 779 records obtained under clear-sky conditions (0 okta of TCC as threshold). The y and x axis represent the length and the
 780 first year of the period under analysis, respectively, while the colored pixels show the trend expressed in %/decade with
 781 a significance level $p \leq 0.1$ (large squares) and $p > 0.1$ (small squares).
 782



783

784 Fig. 8. All-sky (black lines) and clear-sky 0 okta (red lines) SSR annual and seasonal low-pass filter for Northern (left
 785 column) and Southern (right column) Italy. The filters are the same as in Fig. 4 and Fig. 6.